

เส้นโค้งลักษณะเฉพาะที่ไบแอสต่ำของรอยต่อโลหะกับแกลเลียมอาร์เซไนด์ที่ถูกเจือปนอย่างมาก

นาย ประธาน ศรีวิไล



วิทยานิพนธ์นี้เป็นส่วนหนึ่งของการศึกษาตามหลักสูตรปริญญาวิทยาศาสตรมหาบัณฑิต
สาขาวิชาฟิสิกส์ ภาควิชาฟิสิกส์
บัณฑิตวิทยาลัย จุฬาลงกรณ์มหาวิทยาลัย

ปีการศึกษา-2542

ISBN 976-333-080-1

ลิขสิทธิ์ของบัณฑิตวิทยาลัย จุฬาลงกรณ์มหาวิทยาลัย

**CHARACTERISTIC CURVE AT LOW BIAS OF A HEAVILY DOPED
GaAs AND METAL JUNCTION**



Mr. PRATHAN SRIVILAI

A Thesis Submitted in Partial Fulfillment of the Requirements

for the Degree of Master of Science in Physics

Department of Physics

Graduate School Chulalongkorn University

Academic Year 1999

ISBN 976-333-080-1

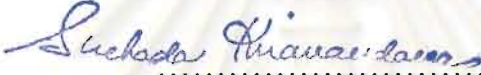
Thesis Title CHARACTERISTIC CURVE AT LOW BIAS OF
 A HEAVILY DOPED GaAs AND METAL
 JUNCTION

By Mr. Prathan Srivilai


Department Physics


Thesis Advisor Associate Professor Wichit Sritrakool, Ph.D.


Accepted by the Graduate School, Chulalongkorn University in
Partial Fulfillment of the Requirements for the Degree of Master of
Science in Physics.


.....Dean of Graduate School
(Associate Professor Suchada Kiranandana, Ph.D.)

Thesis Committee


.....Chairman
(Professor Virulh Sa-yakanit, F.D.)


.....Thesis Advisor
(Associate Professor Wichit Sritrakool, Ph.D.)


.....Member
(Assistant Professor Kajornyod Yoodee, Ph.D.)


.....Member
(Associate Professor Mayuree Natenapit, Ph.D.)

ประธาน ศรีวิไล : เส้นโค้งลักษณะเฉพาะที่ไบแอสต่ำของรอยต่อโลหะกับ
แกเลียมอาร์เซไนด์ที่ถูกเจือปนอย่างมาก (CHARACTERISTIC CURVE AT
LOW BIAS OF A HEAVILY DOPED GaAs AND METAL JUNCTION)

อาจารย์ที่ปรึกษา : รองศาสตราจารย์ ดร. วิชิต ศรีตระกูล,

74หน้า. ISBN 974-333-080-1

เราได้คำนวณค่าที่เกิดขึ้นภายในรอยต่อระหว่างโลหะกับแกเลียมอาร์เซ-
ไนด์ (GaAs) ชนิดเอ็นที่ถูกเจือปนอย่างมากจากสมการของฟิวชองโดยคำนึงถึงพาหะ
ข้างมากร่วมด้วย ดังนั้นในกรณีที่สารกึ่งตัวนำถูกเจือปนอย่างมาก(ความหนาแน่นของผู้
ให้มากกว่า 5×10^{19} อะตอมต่อลูกบาศก์เซนติเมตร) สามารถประมาณได้ว่าค่าจะลดลง
แบบเอ็กซ์โพเนนเชียล จากนั้นเราจะคำนวณหาเส้นโค้งลักษณะสำคัญของความต่างศักย์กับ
กระแสและความต้านทานของรอยต่อภายใต้เงื่อนไขของฟิลด์อิมิตชันในกรณีที่ความ
สัมพันธ์ระหว่างโมเมนตัมและพลังงานเป็นแบบพาราโบลา นอกจากนี้ในกรณีที่การ
ไบแอสมีค่าต่ำ เรายังได้พิจารณาถึงกรณีที่ความสัมพันธ์ดังกล่าวไม่เป็นแบบพาราโบลา
โดยคำนวณความสัมพันธ์ดังกล่าวจากความหนาแน่นของสถานะของสารกึ่งตัวนำ สุดท้าย
ทำได้แสดงให้เห็นว่าสัมประสิทธิ์การทะลุผ่านของโลคอลไลซ์อิเล็กตรอนสามารถละ
ทิ้งได้เมื่อเปรียบเทียบกับสัมประสิทธิ์การทะลุผ่านของดีโลคอลไลซ์อิเล็กตรอน

สถาบันวิทยบริการ
จุฬาลงกรณ์มหาวิทยาลัย

ภาควิชา
สาขาวิชา
ปีการศึกษา 2542

ลายมือชื่อนิสิต
ลายมือชื่ออาจารย์ที่ปรึกษา
ลายมือชื่ออาจารย์ที่ปรึกษาร่วม

พิมพ์ต้นฉบับบทความวิทยานิพนธ์ภายในกรอบสี่เหลี่ยมนี้เพียงแผ่นเดียว

3970956123 MAJOR PHYSICS

KEY WORD: HEAVILY DOPED SEMICONDUCTORS / FILED EMISSION / V-I CHARACTERISTIC / CONTACT RESISTANCE

PRATHAN SRIVILAI: CHARACTERISTIC CURVE AT LOW BIAS OF
A HEAVILY DOPED GaAs AND METAL JUNCTION. THESIS

ADVISORS: ASSOCIATED PROFESSOR WICHIT SRITRAKOOL, Ph.D. 74 pp.

ISBN 974-333-080-1

We have determined the electrostatic potential at the junction between a metal and heavily doped n-type GaAs from the Poisson equation by including the majority carriers. At sufficiently high doping (donor concentration larger than 5×10^{19} atoms/cm³), the electrostatic potential can be approximated by an exponential barrier shape. Consequently, the V-I characteristic and contact resistance are calculated by using the field emission and parabolic energy-momentum relationship. At low biases, we have also used the nonparabolic energy-momentum relationship calculated from the density of states. Finally, we can show that, the transmission probabilities of localized electrons is negligible compared to that of delocalized electrons.



ภาควิชา.....
สาขาวิชา.....
ปีการศึกษา..... 2542

ลายมือชื่อนิสิต.....
ลายมือชื่ออาจารย์ที่ปรึกษา.....
ลายมือชื่ออาจารย์ที่ปรึกษาร่วม.....

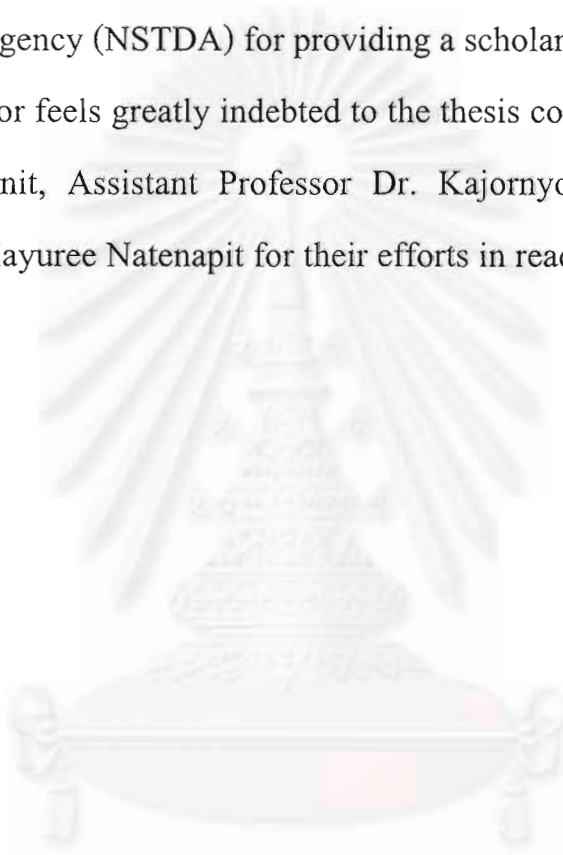
ACKNOWLEDGEMENTS



The author would like to express his gratitude to his advisor Associate Professor Dr. Wichit Srirakool for his invaluable advice, discussion and review this thesis.

He is also grateful to the National Science and Technology Development Agency (NSTDA) for providing a scholarship.

The author feels greatly indebted to the thesis committee, Professor Dr. Virulh Sa-yakanit, Assistant Professor Dr. Kajornyod Yoodee, Associate Professor Dr. Mayuree Natenapit for their efforts in reading and criticizing the manuscript.



สถาบันวิจัยบริการ
จุฬาลงกรณ์มหาวิทยาลัย

TABLE OF CONTENTS

	Page
Abstract in Thai	iv
Abstract in English	v
Acknowledgements	vi
List of Tables	ix
List of Figures	x
List of Symbols	xii
Chapter 1 Introduction	1
Chapter 2 Heavily Doped Semiconductors	4
2.1 Electron and Hole Densities	4
2.2 Fermi Level of Semiconductors	8
2.3 Heavily Doped Semiconductors	10
2.4 Density of States	12
Chapter 3 Current Transport Mechanisms	15
3.1 Formation of Metal-Semiconductor Contact	15
3.2 Voltage-Current Characteristic of Schottky Barriers	19
3.2.2 Transport Properties of Schottky Barrier Made of Lightly Doped Semiconductor.....	21
3.2.2 Transport Properties of Schottky Barrier Made of Heavily Doped Semiconductor.....	25
3.3 Contact Resistance	36
Chapter 4 Field Emission for Parabolic Case	40

4.1 Asymptotic Solution of Poisson's Equation	40
4.2 The V-I Characteristics.....	46
Chapter 5 Field Emission for Nonparabolic Case	57
5.1 The V-I Characteristic Curve	57
5.2. Localized Electron Tunneling	64
Chapter 6 Summary and Discussion	68
References	71
Curriculum Vitae	74



สถาบันวิทยบริการ
จุฬาลงกรณ์มหาวิทยาลัย

LIST OF TABLES

Page

Table 4.1 Work functions and contact potentials for some common metal contacted with GaAs of which electron affinity equal to 4.07 (V).....45



สถาบันวิทยบริการ
จุฬาลงกรณ์มหาวิทยาลัย

LIST OF FIGURES

	Page
Figure 2.1 The Fermi-Dirac distribution function is plotted as a function of the energy when $T > 0$	5
Figure 2.2 Density-of-states function for semiconductor.....	11
Figure 3.1 Formation of barrier between a metal and a semiconductor	15
Figure 3.2 Barriers for semiconductors of difference types and work functions.....	18
Figure 3.3 Transport processes in a forward-biased Schottky barrier.....	20
Figure 3.4 Experimental and theoretical forward-bias current density J versus V for W-Si and W-GaAs diode.....	24
Figure 3.5 Thermionic-field and field emission under forward bias.....	25
Figure 3.6 Potential energy diagram for a tunneling structure.....	28
Figure 3.7 Condition and calculated for Au-GaAs Schottky barrier as a function of the semiconductor impurity concentration.....	32
Figure 3.8 Forward V-I characteristic of a gold heavily doped n-type silicon diode at 77° K.....	33
Figure 3.9 The parabolic (1), Franz (2) , and Kane dispersion relationships as computed for GaAs.....	35
Figure 3.10 Low bias forward characteristic of a Au-n-type GaAs Schottky barrier.....	36
Figure 3.11 Voltage –current characteristics of Schottky barrier diode and of an ohmic contact.....	37
Figure 3.12 Theoretical and experimental values of specific contact	

resistance.....	39
Figure 4.1 Formation of barrier between a metal and a degenerate semiconductor	40
Figure 4.2 Parabolic and exponential potentials for an Au-GaAs junction (GaAs with $N_d = 5 \times 10^{19} \text{ cm}^{-3}$ at 300 K).....	44
Figure 4.3 The relationship of donor concentration (atoms/cm ³) and temperatures calculated for Au-GaAs Schottky barrier	47
Figure 4.4 The relationship (condition (4.19) in thermal energy units) of donor concentration and temperatures calculated for Au-GaAs Schottky barrier at 300K and 77K.....	50
Figure 4.5 The voltage–current characteristics for an Au–GaAs ($N_d = 1 \times 10^{19} \text{ atoms/cm}^3$) diode at 77K in the normal and the log scale.....	52
Figure 4.5 The voltage –current characteristics for Au-GaAs, Al-GaAs, and Cu-GaAs diode ($N_d = 5 \times 10^{19}$) at 77 K.....	53
Figure 4.6 The voltage–current characteristic for an Au-GaAs diode for various doping concentration N_d (donors/cm ³) at 77 K.....	54
Figure 4.7 The voltage–current characteristic for an Au-GaAs diode ($N_d = 1 \times 10^{20} \text{ atoms/cm}^3$) at various temperature.....	55
Figure 4.8 The contact resistance of Au –GaAs in parabolic and exponential barrier approximations at 300K.....	56
Figure 5.1 The quasi momentum (eq. (4.7)) computed for GaAs ($2 \times 10^{19} \text{ donor atoms/cm}^3$)	60
Figure 5.2 The Voltage-current characteristic for Au-GaAs diode ($2 \times 10^{18} \text{ donor atom/cm}^3$) at 77	63
Figure 5.3 Magnitude of k_c versus arbitrary energies of electrons	

of n-type GaAs (2×10^{19} donor atoms/cm³)68



สถาบันวิทยบริการ
จุฬาลงกรณ์มหาวิทยาลัย

List of Symbols

Symbol	Description
A^*	Richardson constant corresponding to effective mass in semiconductor
E	electron energy
E_c	energy at the bottom of conduction band
E_F	Fermi energy
E_F^m	Fermi level in metal
E_F^s	Fermi level in semiconductor
E_g	energy gap of semiconductor
E_v	energy at the top of valence band
$f(E)$	Fermi function
h	Planck's constant
\hbar	Planck's constant divided by 2π
I	current
J	current density
k	wave vector of electron
k_B	Boltzmann's constant
m_e^*	effective mass of an electron in semiconductor
m_h^*	effective mass of a hole in semiconductor
n	density of electrons in conduction band of semiconductor
N_c	effective density of states in conduction band of semiconductor
N_d	donor density
N_v	effective density of states in valence band of semiconductor

p	density of holes in valence band of semiconductor
q	electronic charge
\bar{r}_j	impurity location
R_c	contact resistance
T	absolute temperature or transmission coefficient (eq. (5.19))
V	applied bias (positive for forward bias)
V_{bi}	built in potential or “diffusion voltage”
V_i	drop in potential across interfacial layer
w	width of depletion region
α	defined by eq. (4.8)
α_c	localization parameter
δ	thickness of interfacial layer
ϵ_s	permittivity of semiconductor
ϵ_0	permittivity of free space
ξ	Fermi level in Semiconductor (measured from E_c , $E_f' - E_c$)
ρ	charge density
ϕ	electrostatic potential
ϕ_b	height of Schottky barrier
$q\phi_m$	work function of metal
$q\phi_s$	work function of semiconductor
$q\phi_n$	energy interval between conduction band and Fermi level in equilibrium
χ_s	electron affinity of semiconductor

Chapter1

Introduction



The metal-Semiconductor contact has been in existence for more than a hundred years. Braun (1874) was the first person who can describe the rectifying properties of a thin wire brought in contact with a variety of natural crystals. These point-contact rectifiers of various kinds found practical applications in early day's radio telegraphy, although the rectification mechanism was not understood.

The first step towards understanding the rectifying action of metal-semiconductor contacts was taken in 1931, when Schottky, Stormer, and Waible showed that it was a current flow then the potential drop occurs almost entirely at the contact, there by implying the existence of some sort of potential barrier. In 1938 Schottky and, independently, Mott pointed out that the observed direction of rectification could be explained by supposing that electrons passed over a potential barrier through the normal processes of drift and diffusion. A significant advance in our understanding of metal-semiconductor contacts came during the Second World War as a result of the use of silicon and germanium point-contact rectifiers in microwave radars. This advance was considerably helped by developments in semiconductor physics. The realization that evaporation of metal films in high vacuum system produced contacts which were much more stable and reproducible than point-contacts triggered off a great flurry of a activity in the 1950s and 1960s and laid the foundation for our present extensive knowledge of the

subject. This activity was inspired to a considerable extent by the great importance of contact in semiconductor technology.

Metal-semiconductor contacts are important in microwave applications and as tools in the analysis of other fundamental physical parameters. Most of these applications are based on the interpretation or use of the electron transport properties of the particular barrier considered. This is the reason why understanding of the voltage-current characteristic is one of the important aspects of the study of metal-semiconductor contacts.

For a heavily doped semiconductor or for operation at low temperatures, especially in semiconductors with small electron effective mass, such as GaAs, the tunneling current will become the dominant transport process, such a mechanism is called “field emission”. When we consider the case of the depletion approximation. In this approximation the free-carrier density is assumed to fall abruptly from a value equal to that density in the bulk semiconductor to a value negligible compared to the donor or acceptor concentration. In more accurately than the depletion approximation, we must allow for the fact the majority carrier concentration does not fall abruptly to zero but penetrates in to the depletion region. Then, in Chapter 4 we account for the majority carriers in the charge density and solve Poisson’s equation in case of a degenerate semiconductor. We obtain the electrostatic potential. As a result, based on the field emission, the voltage-current characteristic can be calculated. In this thesis, we are interested in the V-I characteristic at low bias. Consequently, the Schottky effect, and the emission of electron over the top of the potential barrier can be neglected.

In case of barriers such as the one made by an n-type GaAs, the electrons experience a highly nonparabolic energy-momentum relationship when tunneling through the energy gap at low biases. The influence of nonparabolic energy-momentum relation on V-I characteristic of tunneling junction was first considered by Padovani and Stratton^[1]. The electron energy-momentum relationship in the forbidden gap can be calculated using Kane's two-band model and Franz's empirical expression. In Chapter 5, we present our calculations for the electron energy-momentum relationship in the forbidden gap (accounting tail states). As a result, V-I characteristic at low bias of heavily doped GaAs can be calculated, and we compare the localized electron transmission probability with the delocalized electron transmission probability in the last section. We review some basic theories of heavily doped semiconductors in Chapter 2, and current transport mechanisms, especially in field emission regime, in Chapter 3. Finally, discussion and conclusion are given in Chapter 6.

Chapter 2

Heavily Doped Semiconductors

The physics of metal-semiconductor contacts is naturally dependent on the physics of semiconductors themselves. This chapter presents a summary of the physics and properties of semiconductors.

2.1 Electron and Hole Densities ^[2]

Electrons in a solid obey the Pauli exclusion principle and are indistinguishable in their characteristics. Each available state contains two electrons of opposite spin angular momentum. The statistics governing the energy-level occupation is the Fermi-Dirac given by the Fermi function

$$f(E) = \frac{1}{1 + \exp[(E - E_f)/k_b T]} \quad (2.1)$$

where E_f is the Fermi energy. As usual, Eq.(2.1) gives the probability of finding an electron in the energy state E . Some simple observations about this function will remind us its application to some physical problems of electron occupancy.

At the absolute zero of temperature, all electron states have unity probability of being filled for $E < E_f$, and the states of which $E > E_f$ are completely empty. Thus the Fermi-Dirac distribution is a “reversed Heaviside” function; it is unity up to the Fermi level and zero for energies beyond the Fermi level. At higher temperatures, there is gradual spreading of the distribution about the Fermi level. as shown in Fig. 2.1.

The electrons that would normally exist in the region marked “ $T = 0$ ” are excited to the region marked “ $T > 0$ ”. The number of electrons transferred from below the Fermi energy to above the Fermi energy are given by the marked areas weighted by the appropriate density of states function. The Fermi energy must adjust so that the number of electrons removed from area $T = 0$ is exactly equal to number of electrons excited into area $T > 0$. In an intrinsic semiconductor, this means that the Fermi level will be somewhere near midgap, but this is not the case in an impurity-dominated semiconductor. It is just the Fermi energy position, one of the crucial factors, that must be determined in next section.

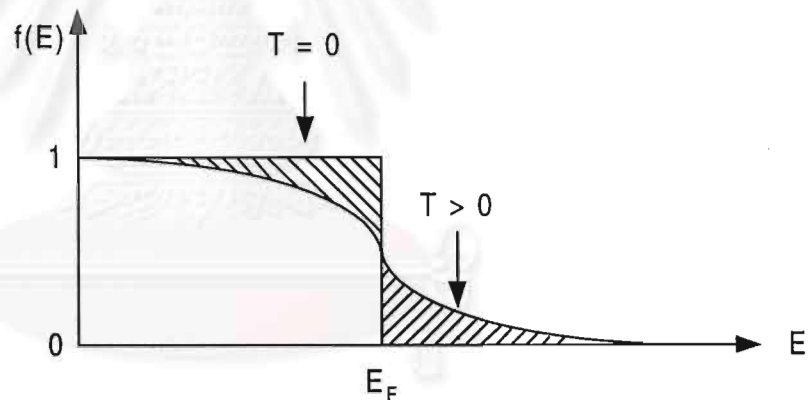


Fig. 2.1 The Fermi-Dirac distribution function is plotted as a function of the energy when $T > 0$.

The total number of electrons in a band given by the sum over all of the possible energy states that exist in the band, while each of the states is weighted by the probability that it is filled, or for the conduction band,

$$n = \int_{E_c}^{\infty} N(E) f(E) dE \quad (2.2)$$

where E_c is the lower edge of the conduction band. Thus, to a particular density of electrons in the conduction band, there is a very specific value of the Fermi energy that is required in order to satisfy eq.(2.2). The density of states function $N(E)$ is free electron approximation

$$N(E) = \frac{1}{2\pi^2} \left(\frac{2m_e^*}{\hbar^2} \right)^{3/2} (E - E_c)^{1/2} \quad (2.3)$$

where m_e^* is the density-of-states effective mass. Equations (2.1) and (2.3) can be combined to yield

$$n = \frac{1}{2\pi^2} \left(\frac{2m_e^*}{\hbar^2} \right)^{3/2} \int_0^{\infty} \frac{(E - E_c)^{1/2}}{1 + \exp[(E - E_f)/k_B T]} dE \quad (2.4)$$

where the zero of energy has been shifted to the conduction-band edge (E_c). Equation (2.4) was obtained by neglecting the state energies lying below the conduction-band edge (absent of the tail states).

In eq.(2.4), for a large electron density n , the Fermi energy can be expected to lie within the conduction band. This case is termed the degenerate limit, and the full form of the Fermi-Dirac function is required in the integral. Where the temperature is not too low and the density is not too high, eq. 2.4 can be satisfied with the situation when the Fermi energy lying within the forbidden energy gap so that only the tail of the Fermi-Dirac function extends into the conduction band. In this case only a small fraction of the states are occupied, even for the lowest energies in the band. All occupied states lie near the band edge, and the electron density with its statistics are termed nondegenerate. In the latter case, its statistics is termed classical, as

$$\left(1 + \exp\left[\frac{E - E_f}{k_b T}\right]\right)^{-1} \approx \exp(-(E - E_f)/k_b T) \quad (2.5)$$

for the conduction band states. This approximation usually requires the Fermi energy to lie some 3 to 5 times of $k_b T$ below the conduction-band edge. The electron density in this case is relatively small.

By introducing a set of reduced variables for the energies:

$$y = \frac{E - E_c}{k_b T}, \quad \eta = \frac{E_f - E_c}{k_b T}, \quad (2.6)$$

the density in eq.(2.4) becomes

$$n = \frac{1}{2\pi^2} \left(\frac{2m_c k_b T}{\hbar^2}\right)^{3/2} \int_0^\infty \frac{y^{1/2}}{1 + \exp[y - \eta]} dy \equiv N_c F_{1/2}(\eta) \quad (2.7)$$

In this last formulation, the Fermi-Dirac integral is introduced through its definition

$$F_j(\eta) = \frac{2}{\Gamma(j+1)} \int_0^\infty \frac{y^j}{1 + \exp[y - \eta]} dy \quad (2.8)$$

and the effective density of states is defined as

$$N_c = 2 \left(\frac{2\pi m_c k_b T}{h^2}\right)^{3/2}. \quad (2.9)$$

The latter quantity is quite important, as it is the number of electrons per unit volume that will exist in the conduction band if it is assumed that a density is localized at the edge. In essence, it tells us whether or not a degenerate

system exists. If $n \ll N_c$, the density is nondegenerate, but if $n \gg N_c$, the statistics is degenerate. In a similar manner, the case of holes in the valance band can be developed. However, for holes, the probability is that corresponding to an empty state; for example.

$$f_h(E) = 1 - f_e(E) \quad (2.10)$$

where $f_h(E)$ and $f_e(E)$ are the Fermi-Dirac functions for holes and electrons, respectively. The density of holes is then given by

$$\begin{aligned} p &= \int_{-\infty}^{E_v} N_v(E) f_h(E) dE \\ &= N_v F_{1/2}(\eta_h) \end{aligned} \quad (2.11)$$

where $y = \frac{E - E_v}{k_B T}$, $\eta_h = \frac{E_F - E_v}{k_B T}$, m_h^* is the density-of-state effective mass for the valance band and including both light and heavy holes and

$$N_v = 2 \left(\frac{2\pi m_h^* k_B T}{h^2} \right)^{3/2}. \quad (2.12)$$

2.2 Fermi Level in Semiconductors

Closed-form solutions for the Fermi-Dirac integrals do not exist for the case in which the argument is larger than zero. Asymptotic expansions also exist for a large positive argument (i.e., the integral is integrated up to the argument and the denominator in eq.(2.8) is set equal to unity). For large negative arguments the integral is closely approximated to the Maxwell-Boltzmann distribution function. Since the latter case is the one that arises

for nondegenerate semiconductors and therefore has relatively great applicability, the latter case will be treated more extensively. Then the Fermi-Dirac integral is just

$$F_{1/2}(\eta) \approx \exp[\eta]. \quad (2.13)$$

Substituting eq. (2.13) in eq. (2.7), we obtain

$$n \approx N_c \exp[(E_f - E_c)/k_b T] \quad (2.14)$$

In the opposite limiting case, when the Fermi level enters the conduction (or the valance) band, the semiconductor is called degenerate semiconductor.

In this case

$$F_{1/2}(\eta) \approx \frac{4}{3\sqrt{\pi}} \eta^{3/2}, \quad (2.15)$$

$$n \approx N_c \left(\frac{4}{3\sqrt{\pi}} \eta^{3/2} \right). \quad (2.16)$$

The position of the Fermi level, E_f , can be found from the condition of neutrality:

$$p + \sum_j Z_j N_j - n = 0 \quad (2.17)$$

where Z_j is the charge (in units of the electron charge) of an impurity of type j and N_j is the concentration of such impurities. In case of heavily doped n-type semiconductors, it is found from eq. (2.17) that

$$n = N_d \quad (2.18)$$

the position of the Fermi level is found from the equation

$$N_c F_{1/2}(\eta) = N_d. \quad (2.19)$$

For degenerate semiconductors ($\eta \gg 1$) it is found that

$$E_f - E_c = \frac{\hbar^2}{2m_n^*} (3\pi^2 N_d)^{2/3}. \quad (2.20)$$

This result may also be obtained in a simple way by counting the number of allowed states in the Fermi sphere.

2.2 Heavily Doped Semiconductors^[4]

In extrinsic semiconductors with low impurity concentrations, it is generally assumed that the conduction and valence-band edges as well as the donor and acceptor-state energies are sharply defined. These energies coincide with their respective positions in the intrinsic material. In a degenerate semiconductor, however, we must take into account modifications introduced into the band structure by heavy impurity concentrations. The two effects of high doping can be described as follows. First, the hydrogen-like impurity-atom wave functions begin to overlap. As a result, the energy of the impurities broadens to form a band, known as the impurity band. Second, an impurity atom introduces a local variation in the potential energy of an electron because of the difference in the nuclear potential of the impurity and host atom.

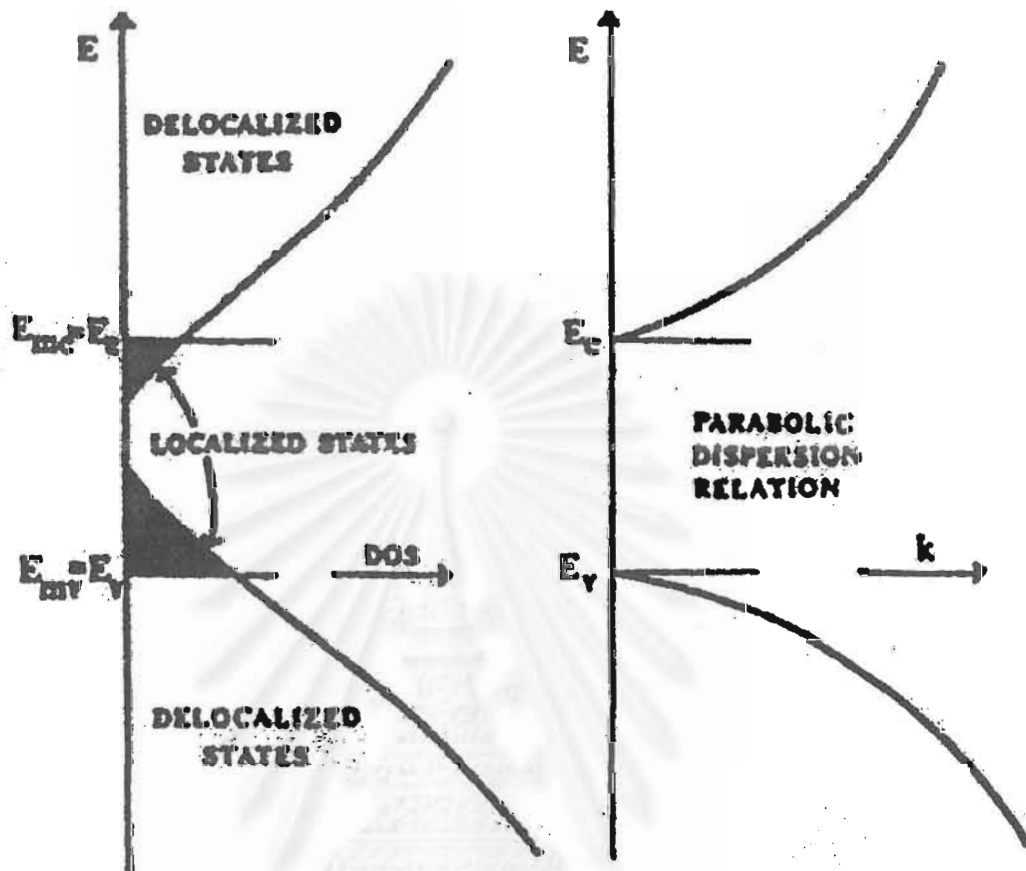


Fig.2.2 Schematic representation of the band structure showing (on the left) localized states in the band tail between E_v and E_c and delocalized states outside this range. On the right the parabolic DOS used to describe the delocalized states above the mobility edge $E_{mc} = E_c$ and below $E_{mv} = E_v$ is shown ^[5].

Such a local, random variation in the potential energy modifies the position of the band edges. As a result, the bands extend beyond their respective positions in the intrinsic material. The extended part of a band is called the band tailing. In Fig. 2.2, the band structure of a heavily doped

semiconductor is drawn for comparison with the band structure of the intrinsic material.

2.3 Density of States (DOS)^[6]

We begin with free electrons. In this case the electron wave function are plane waves corresponding to parabolic momentum-energy relationship. The density of states per unit volume at energy E is defined as

$$\rho(E) = \frac{1}{V} \sum_{\vec{k}} \delta(E - E_{\vec{k}}) \quad (2.22)$$

where the sum is over the free electron energies $E_{\vec{k}}$. Taking V large, we may convert the sum over \vec{k} to an integral and use a property of the delta function to go

$$\rho(E) = \frac{m^{3/2}}{\sqrt{2\pi^2 \hbar^3}} E^{1/2} H(E) \quad (2.23)$$

where $H(E)$ is the heaviside step function defined as

$$H(E) = \begin{cases} 1 & E > 0 \\ 0 & E < 0. \end{cases} \quad (2.24)$$

For an undoped semiconductor, the DOS has a parabolic shape with E so that it is always called the “parabolic” DOS.

For a heavily doped semiconductor, Kane^[7] has combined the potential energy fluctuations with the Thomas-Fermi method or semi-classical methods, to calculate the density of states. In this method he assumes that the

potential is sufficiently slowly varying from place to place in the crystal that a local density of states can be defined just as if the potential were constant. The calculation of the total density of states then reduces to the calculation of the distribution function of the potential. It was noticed that the potential energy distribution at high concentration is Gaussian and the resulting band tail found by Kane is Gaussian.

In Kane's theory, the DOS is written in terms of the well-known parabolic cylinder function $D_p(z)$ as

$$\rho(E) = \frac{m^{*3/2}}{4\pi^2 \hbar^3} \xi_0^{1/4} \exp\left[\frac{(E - E^*)^2}{4\xi_0}\right] D_{-3/2}\left(\frac{-(E - E^*)}{\sqrt{\xi_0}}\right) \quad (2.25)$$

here E^* is the averaged potential and ξ_0 is the potential fluctuation defined by the equation

$$\xi_0 = \frac{2\pi Z^2 e^4 N}{Q \epsilon_s^2} \quad (2.26)$$

where ϵ_s is the semiconductor permittivity and Q is the inverse screening length defined by the equation

$$Q^2 = \frac{4m^* e^2}{\epsilon_s \hbar^2} \left(\frac{3N}{\pi}\right)^{1/3} \quad (2.27)$$

N in eq.(2.26) is the number of impurities of charge Z . For large E eq.(2.25) approaches the limit of free electrons. The Kane DOS at very deep tail region where $E - E^*$ is large and negative is a function of $\exp[-E^2]$.

The most complete calculation of density of states in the low energy, deep tail region of the impurity-band, remains the optimal fluctuation results of Halperin and Lax theory. Their theory is the quantum counterpart of the original semi-classical theory of Kane. Quantum effects were included by adding the zero point energy of electron states (kinetic energy of localization) which raises the electron state energies and reduces the density of states at small energy below the semiclassical value obtained by Kane. However, their $\rho(E)$ is obtained as a numerical table and is not easy to use.

Sa-yakanit and Glyde (SG), have used the Feynman path integral technique to obtain an expression for $\rho(E)$ valid at all E . This expression reduces to simple form in the band-tail region (low E) and reduces to expected parabolic value at high E . Since SG's DOS^[8] is obtained by modelling impurity fluctuation wells by harmonic wells and the model gives Gaussian wave functions. Our envelope function^[5] is assumed to be of a Gaussian form instead of a hydrogenic atom form. The envelope function for the electrons in the conduction band is

$$\psi_c(\vec{k}_c, \vec{r}) = \left(\frac{2\alpha_c}{\pi}\right)^{3/4} \exp[i\vec{k}_c \cdot \vec{r}] \exp[-\alpha_c |\vec{r} - \vec{r}_j|^2] \quad (2.28)$$

where \vec{r}_j is the impurity location and the localization parameter (α_c) is related to the variational parameter z_c calculated by Sritrakool et.al^[9] by the relation

$$\alpha_c = \frac{Q^2}{2z_c^2} \quad (2.29)$$

the values of the parameter z_c for heavily doped GaAs.

Chapter3

Current-Transport Mechanisms

This chapter discusses the transport mechanisms which determine the conduction properties of metal-semiconductor contacts. In the first part, the V-I characteristic of Schottky barriers made on low concentration semiconductors will be discussed. In the second part, the V-I characteristic of Schottky barriers made on highly doped semiconductors material will be discussed in terms of electron tunneling through the barrier.

3.1 Formation of Metal-Semiconductor Contact

3.1.1 Idealized Metal - Semiconductor Contact

To see how a metal-semiconductor contact may form when a metal comes into contact with a semiconductor, we suppose that the metal and semiconductor are both electrically neutral and separated from each other. The energy band diagram is shown in Fig.3.1 (a) for an n-type semiconductor with a work function ϕ_m less than that of the metal. This is the most important case in practice, and it is supposed that there is no surface state present. If the metal and semiconductor are connected electrically by a wire, electrons pass from the semiconductor into the metal and the two Fermi levels are forced to coincide as shown in Fig 3.1 (b). The positive charges are provided by conduction electrons receding from the surface, leaving uncompensated positive donor ions in a region depleted of electrons. Because the donor concentration is many order of magnitude less than the concentration of electrons in metal, the uncompensated donors occupy

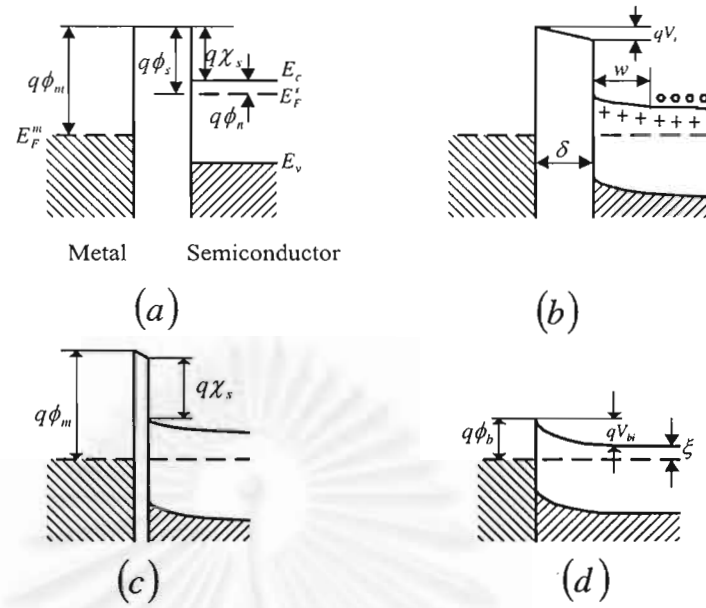


Fig. 3.1 Formation of barrier between a metal and a semiconductor (a) neutral and isolated, (b) electrically connected, (c) separated by a narrow gap, (d) in perfect contact. The symbol \circ denotes electrons in conduction band and $+$ denote donor ions^[2].

A layer of appreciable thickness W . If the metal and semiconductor approach each other, qV_i must tend to zero if the field in the gap is to remain finite [Fig. 3.1(c)] and where they finally touch [Fig. 3.1 (d)], the barrier due to vacuum disappears altogether and we are left with an ideal metal-semiconductor contact. It is clear from the fact that V_i tends to zero so that the height of the barrier (ϕ_b) measured relative to the Fermi level is given by

$$\phi_b = \phi_m - \chi_s. \quad (3.1)$$

In most practical metal-semiconductor contacts, the ideal situation shown in Fig. 3.1 (d). The foregoing description applies to an n-type semiconductor with work function energy ($q\phi_s$) less than the work function energy ($q\phi_m$) of

the metal. It will be seen later that such a contact behaves as a rectifier. If a similar argument is developed for the case when (ϕ_s) is greater than (ϕ_m) one obtains a band diagram of the form shown in Fig. 3.2 (b). Clearly, if such a contact is biased so that electrons flow from the semiconductor to metal, they encounter no barrier. If it is biased so that electrons flow in the reverse direction, the comparatively high concentration of electrons in the region where the semiconductor bands are bent downwards behave like a cathode which is easily capable of providing a copious supply of electrons. The current is then determined by the bulk resistance of semiconductor. Such a contact is termed an ohmic contact. This type of contact has a sufficiently low resistance for the current to be determined by the resistance of the bulk semiconductor rather than by the properties of the contact.

In a p-type semiconductor for which ϕ_m exceeds ϕ_s , we obtain the band diagram shown in Fig. 3.2 (c), which also represents an ohmic contact. The case of a p-type semiconductor for which ϕ_s exceed ϕ_m is shown in Fig. 3.2 (d). Bearing in mind that holes have difficulties in going underneath a barrier, one sees that Fig. 3.2 (d) is the p-type analogue of Fig. 3.2 (a) and gives rise to rectification. Figure 3.2 (b) and (c) are very uncommon in practice and the majority of metal-semiconductor combinations form rectifying or “blocking” contacts. Thus all subsequent discussions will be the case of n-type semiconductors with $\phi_m > \phi_s$ which is the most important case in practice.

It is frequently necessary to know how the electrostatic potential and electric-field strength in a Schottky barrier depend on the barrier height, bias

voltage, and impurity concentration, and for most purposes it is sufficiently accurate to use an approximation known as the depletion approximation. In this approximation the free-carrier density is assumed to fall abruptly from a value equal to the density in the bulk of the semiconductor to a value which is negligible compared with the donor or acceptor concentration.

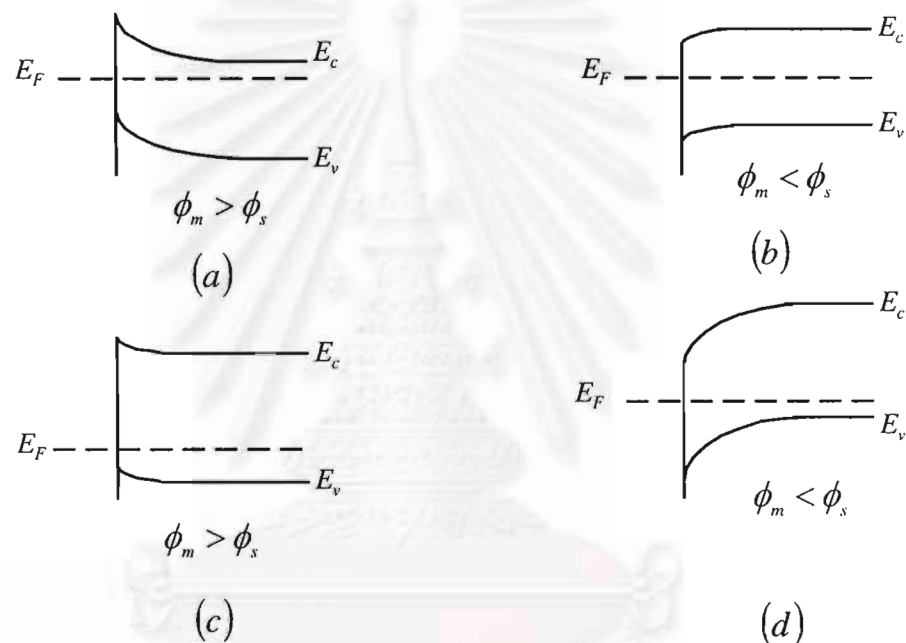


Figure 3.2 Barriers for semiconductors of different types and different work functions. n-type: (a) $\phi_m > \phi_s$ (rectifying); (b) $\phi_m < \phi_s$ (ohmic); p-type: (c) $\phi_m > \phi_s$ (ohmic); (d) $\phi_m < \phi_s$ (rectifying) ^[2].

Let us consider the case of an n-type semiconductor. The charge density and electrostatic potential are related by Poisson's equation

$$\frac{d^2 \phi}{dx^2} = -\frac{\rho(x)}{\epsilon_s} \quad (3.2)$$

where ϵ_s is semiconductor permittivity.

If we take the electrostatic potential $\phi(x)$ to be zero with in the neutral region, so that $\phi(x)$ the potential at x is given by

$$\phi(x) = -\frac{qN_d}{2\epsilon_s}(w-x)^2 \quad (3.3)$$

and

$$w^2 = \frac{2\epsilon_s\phi_b}{qN_d} \quad (3.4)$$

where $\phi(x)$ at the interface is equal to the diffusion potential ϕ_b and w depletion width. The energy of the bottom of the conduction band relative to the Fermi level in the metal is given by

$$E_c(x) = q(\phi_b + \phi(0) + \phi(x)) \quad (3.5)$$

we obtained

$$E_c(x) = \frac{q^2N_d}{2\epsilon_s}(w-x)^2 \quad (3.6)$$

Several effects will alter the actual Schottky barrier height from the theoretical value given by eq.(3.1) such as the effects of surface (or interface) states seen in generalized analysis of Bardeen model (see Rhoderich^[2]). Schottky effect, or image-force-induced lowering of the potential energy for charge carrier emission when an electric field is applied. (see Sze^[10]).

3.2 Voltage- Current Characteristic of Schottky Barriers

The transport mechanisms which determine the conduction properties of Schottky barrier can proceed in different ways. A way in which electrons can be transported across a metal-semiconductor junction under a forward

bias are shown schematically for n-type semiconductors in Fig.3.3. An inverse process occurs under a reverse bias. The mechanisms are :

- Emission of electron from the semiconductor over the top of barrier into the metal; (the dominant process for Schottky diodes made of low doped semiconductors (e.g. Si with $N_d \leq 10^{17} \text{ cm}^{-3}$ operated at moderated temperatures (e.g. 300 K),
- Quantum mechanical tunneling through the barrier (important for heavily doped semiconductors and responsible for most ohmic contacts),
- Recombination in the space-charge region,
- Recombination in neutral region (hole injection).

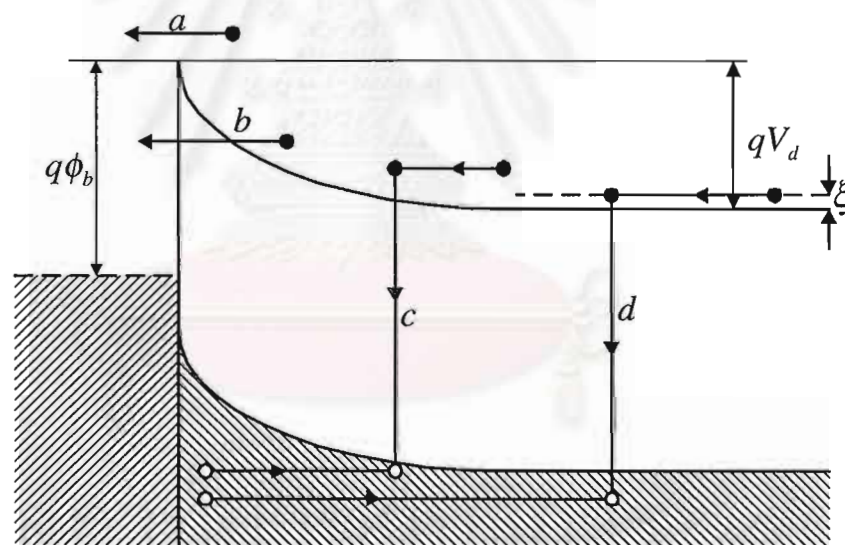


Fig.3.3 Four various transport processes in a forward-biased Schottky barrier^[2]

3.2.1 Transport Properties of Schottky Barrier of Lightly Doped Semiconductor

The activation of charge carrier over the barrier can proceed in two different ways. The choice between the two depends upon the width of the depletion region with respect to the mean free path of electrons scattered by acoustic phonons. If the barrier thickness is small compared with the electron mean free path, collisions can be neglected for all practical purposes. This situation was first considered by Bethe^[10] (i.e. “diode theory”). If the barrier thickness is large compared with the electron mean free path, a carrier experiences many collisions in the barrier region before reaching the top of barrier. This latter case was studied by Wagner, Schottky and Spence^[11], and is usually referred to as the “diffusion” theory.

Thermionic Emission Theory

The thermionic emission theory by Bethe is derived from the assumptions:

- 1) The barrier height ($q\phi_b$) is much larger than k_bT ,
- 2) Thermal equilibrium is established at the plane that determines emission,
- 3) The existence of a net current flow does not affect this equilibrium.

The current density from semiconductor to metal $J_{S \rightarrow M}$ is the concentration of electrons with energies sufficient to overcome the potential barrier and traversing in the x direction, i.e.

$$J_{S \rightarrow M} = \int_{E_F + q\phi_b}^{\infty} qv_x dn \quad (3.7)$$

where $E_F + q\phi_b$ is the minimum energy required for thermionic emission into the metal. And v_x is carrier velocity in direction of transport. If we postulate that all the energy of electrons in conduction band is kinetic energy. We obtain

$$J_{s \rightarrow m} = A^* T^2 \exp\left[\frac{-q(\phi_b - V)}{k_b T}\right] \quad (3.8)$$

where ϕ_b is the barrier height, V is bias voltage and

$$A^* = \frac{4\pi q m^* (k_b T)^2}{h^3} \quad (3.9)$$

is the effective Richardson constant for the thermionic emission and m^* is the effective mass of semiconductor.

The barrier height for electrons moving from the metal into the semiconductor remains the same, the current flowing into the semiconductor is thus unaffected by the applied voltage. It must therefore be equal to the current flowing from the semiconductor into the metal when thermal equilibrium (i.e. when $V = 0$). The corresponding current density is obtained from eq.(3.8) by setting $V = 0$

$$J_{m \rightarrow s} = -A^* T^2 \exp\left[\frac{-q(\phi_b)}{k_b T}\right]. \quad (3.10)$$

The total current density is given by the sum of eq.(3.8) and eq.(3.10),

$$J = J_s \left[\exp\left[\frac{qV}{k_b T}\right] - 1 \right] \quad (3.11)$$

where

$$J_{st} = A T^2 \exp\left[-\frac{q\phi_b}{k_b T}\right]. \quad (3.12)$$

Eq. (3.11) is similar to the transport equation for diodes (The mathematical details can be found in reference [10])

Diffusion Theory

The diffusion theory by Schottky is derived from the assumptions that

- 1) The barrier height is much larger than $k_b T$,
- 2) The effect of electron collisions within the depletion region is included,
- 3) The carrier concentration at $x = 0$ and $x = w$ are unaffected by the current flow,
- 4) The impurity concentration of the semiconductor is nondegenerate.

For Schottky barriers, neglect image-force effect^[10], we obtain

$$J = J_{sd} \left[\exp\left[\frac{qV}{k_b T}\right] - 1 \right] \quad (3.13)$$

where

$$j_{sd} = \frac{q^2 D_n N_c}{k_b T} \left(\frac{2q(\phi_b - V)N_d}{\epsilon_s} \right)^{1/2} \left[\exp\left[\frac{-q\phi_b}{k_b T}\right] \right] \quad (3.14)$$

The current density expressions of the diffusion and thermionic emission theories, are basically very similar. However, the “saturation current density” J_{sd} for the diffusion theory varies more rapidly with the voltage but is less sensitive to temperatures compared with the “saturation current density” J_{st} of thermionic emission theory.

The forward-bias current-voltage characteristics of two Schottky diodes are shown in Fig.3.4 when the forward bias voltage V is greater than

$\frac{4k_n T}{q}$, we can neglect the (-1) term in the diode equation (eq. (3.13)). We

have the $\ln J$ versus V curve as a straight line shown in the Fig. 3.4.

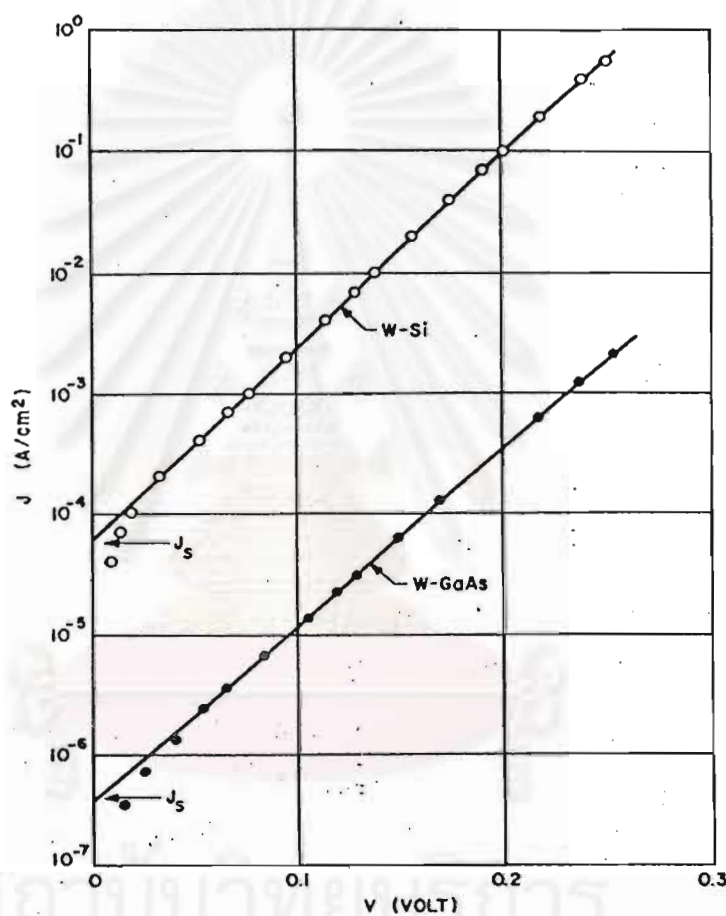


Fig. 3.4 Experimental (dots) and theoretical (solid lines) forward-bias current density J versus V for W-Si and W-GaAs diodes ^[10].

3.2.2 Transport Properties of Schottky Barrier Made of Heavily Doped Semiconductor

For Schottky barrier of highly doped semiconductors, the depletion region becomes so narrow that electrons can tunnel through the barrier well near the top, where the barrier is thin. This process is called thermionic-field. The number of electrons with a given energy E exponentially decreases with energy as $\exp\left[-\frac{E}{k_b T}\right]$ and the transmission coefficient of the barrier exponentially increases with the decrease in the barrier width (see WKB approximation^[11,12]). Hence, the dominant electrons tunneling paths occur at lower energies as doping increases and the barrier becomes thinner. In degenerate semiconductors, especially in semiconductors with small electron effective mass, such as GaAs, electrons can tunnel through the barrier near the Fermi level, and the tunneling current is dominant such a mechanism is called field emission.

Thermionic-Field Emission

The current-voltage characteristic of a Schottky diode in the case of thermionic-field emission can be calculated by evaluating the product of the transmission coefficient and the number of electrons as the function of energy and integrating over the states in the conduction band. Such a calculation yields^[13]

$$J = J_{STF} \exp\left[\frac{qV}{E_s}\right] \quad (3.16)$$

where
$$E_s = E_{\infty} \coth\left(\frac{E_{\infty}}{k_b T}\right), \quad (3.17)$$

and
$$E_{\infty} = \frac{q\hbar}{2} \left(\frac{N_d}{\epsilon_s m^*} \right)^{1/2}. \quad (3.18)$$

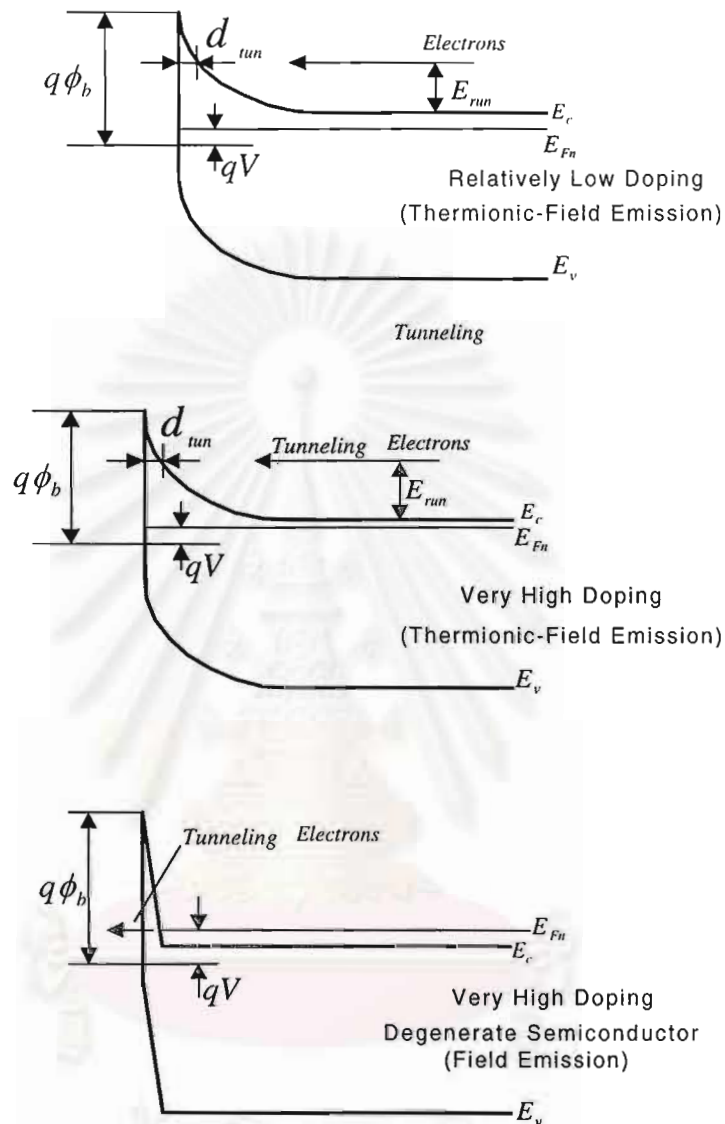


Fig 3.5 Thermionic-field and field emission under forward bias. d_{tun} is the characteristic tunneling length. At low doping electrons tunnel across the barrier closer to the top of the barrier. With increasing in doping, the characteristic tunneling energy, E_{tun} decreases. In highly doped degenerate semiconductors, electrons near the Fermi level tunnel across a very thin depletion region^[13].

The preexponential term was calculated by Crowell and Rideout^[13]:

$$J_{STF} = \frac{A^* T [\pi E_{\infty} q (\phi_b - V + \xi)]^{1/2}}{k_B \cosh\left(\frac{E_{\infty}}{k_B T}\right)} \exp\left[\frac{-q\xi}{k_B T} - \frac{q(\phi_b + \xi)}{E_{\infty}}\right] \quad (3.19)$$

here $\xi = (E_f - E_c)/q$, so that ξ is negative for nondegenerate semiconductors. In GaAs the thermionic field emission occurs roughly when $N_d > 10^{17} \text{ cm}^{-3}$ at 300 K and when $N_d > 10^{16} \text{ cm}^{-3}$ at 77 K. In silicon the corresponding values of N_d are several times bigger.

Field Emission

The quantum mechanical tunneling through the barrier (important for heavily doped semiconductors and responsible for most ohmic contacts), Figure 3.6 shows the potential energy diagram and serves to define the symbols that will be used in the tunnel equation. This can be written as

$$J = \frac{2q}{h^3} \int_0^{\infty} [f_1(E_1) - f_2(E_2)] v_{1x} P(E_1) d^3 p_1 \quad (3.20)$$

where $f_1(E_1)$ and $f_2(E_2)$ are Fermi functions for electrons of energy E_1 and E_2 in conductors 1 and 2, respectively. v_{1x} is the group velocity and $P(E_1)$ is the transmission probability for electrons of energy E_1 . It will be assumed that the WKB approximation is applicable. In addition, the electron energy-momentum relation will be assumed in each of three regions. At sufficiently highly doped semiconductor, the tunneling probability will be greatest for electrons near the Fermi level Padovani and Stratton^[15] have shown that, making Taylor expansions for the transmission probability around the Fermi level of conductor 1 eq.(3.20) leads to

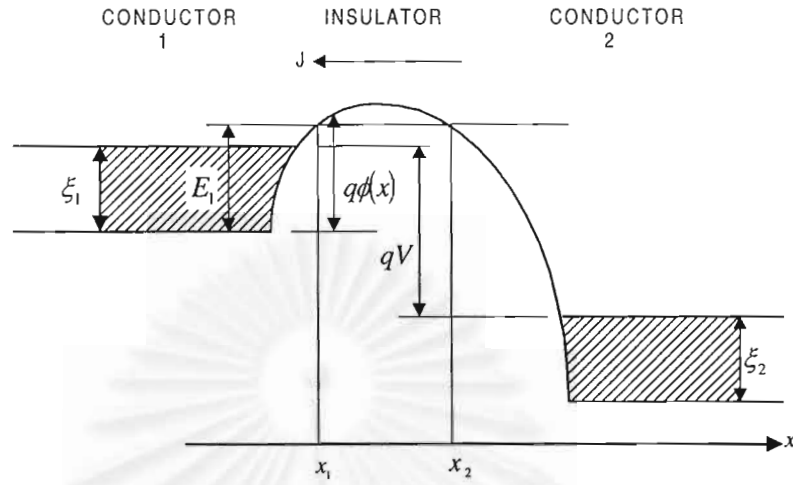


Fig. 3.6 Potential energy diagram for a tunneling structure. The insulating region represents either an insulation film sandwiched between two conductors or a space charge barrier formed at the contact between a metal and semiconductor^[14].

$$J = \frac{2\pi qp_{01F}}{h^3} \exp[-b_{1F}] \int_0^{\infty} [f_1(E_1) - f_2(E_1)] \exp[c_{1F}(E_1 - \xi_1)] dE_1 \left(1 - \frac{1}{2\pi} \int_0^{2\pi} \exp\left[\frac{p_m}{p_{01F}}\right] d\phi\right) \quad (3.21)$$

where $E_2 = E_1 + V + \xi_2 - \xi_1$, under the condition that

$$\frac{1}{k_B T} - c_{1F} > (2f_{1F})^{1/2} \quad (3.22)$$

The coefficients p_{01F} , b_{1F} , c_{1F} and f_{1F} arise in Taylor's expansion of the logarithm of the transmission coefficient around the Fermi level of conductor 1 and are given by

$$\frac{1}{p_{01F}^2} = \frac{1}{\hbar} \int_{x_1}^{x_2} \frac{dx}{(\bar{p})_{\xi}} \quad (3.23)$$

$$b_{1F} = \frac{2}{\hbar} \int_{x_1}^{x_2} (\bar{p})_{\xi} dx \quad (3.24)$$

$$c_{1f} = \frac{2}{\hbar} \int_{x_1}^{x_2} (d\bar{p} / dE)_\xi dx \quad (3.25)$$

$$f_{1f} = \frac{1}{\hbar} \int_{x_1}^{x_2} (d^2\bar{p} / dE^2)_\xi dx \quad (3.26)$$

$-\bar{p}^2 = p^2$ is the square of the quasi-momentum of electron in the forbidden gap of the insulator and $p_m(E_1, \varphi)$ is the maximum value of the component of the quasi-momentum parallel to the plane of the insulation region and the transmission coefficient is the maximum value, when $p_m(E_1, \varphi)$ is minimum (eq.3.21). The parabolic energy momentum relations for the conductor and the insulator are assumed,

$$\bar{p}_\xi^2 = 2m_1(E_1 - \xi_1) \quad (3.27)$$

and

$$p_m^2 = \min[2m_1(E_1), 2m_2(E_2)] \quad (3.28)$$

where $\min [a,b]$ refer to the lesser of the quantities a and b, m_i is the effective mass of the insulation and $E_2 = E_1 + V + \xi_2 - \xi_1$. Thus

$$\frac{p_m^2}{p_{01f}^2} = \min\left[\frac{1}{m_i}(2m_1(E_1), 2m_2(E_1 + V + \xi_2 - \xi_1))\right] \quad (3.29)$$

where $p_{01f}^2 = 2m_1 / c_{1f}$.

Let us now consider more specifically tunneling through a Schottky barrier. An energy diagram for such a barrier is shown in Fig. 3.6 with the relevant parameters used in this analysis. In the forward direction we identify conductor 1 and the insulating region with the degenerate semiconductor and the space-charge region, respectively. Thus and if, further

$$E_1 < E_2 \quad (3.30)$$

which will hold for all reasonable values of the parameters

$$\frac{P_m^2}{P_{01F}^2} = c_{1F} E_1. \quad (3.31)$$

here, m_2 is the electron mass in the metal electrode. Equation 3.21 reduces to

$$J = \frac{A'}{(c_{1F} k_B T)^2} \exp[-b_{1F}] \left\{ \left(\frac{\pi c_{1F} k_B T}{\sin(\pi c_{1F} k_B T)} \right) - (1 + c_{1F} \xi_1) \exp[-c_{1F} \xi_1] \right\} \quad (3.32)$$

if $\exp[(\xi_1 - V)/k_B T] \ll 1$, or to

$$J = \frac{A'}{(c_{1F} k_B T)^2} \exp[-b_{1F}] \left\{ \left(\frac{\pi c_{1F} k_B T}{\sin(\pi c_{1F} k_B T)} \right) (1 - \exp[-c_{1F} V]) - c_{1F} V \exp[-c_{1F} \xi_1] \right\} \quad (3.33)$$

if $\exp[(\xi_1 - V)/k_B T] \gg 1$. Here A' is the Richardson constant, equal to $4\pi m^* (k_B T)^2 / h^3$. In the reverse direction, the same conditions apply and the result V-J characteristic is.

$$J = \frac{A'}{(c_{2F} k_B T)^2} \exp[-b_{2F}] \left\{ \left(\frac{\pi c_{2F} k_B T}{\sin(\pi c_{2F} k_B T)} \right) (1 - \exp[c_{2F} V]) + c_{2F} V \exp[-c_{2F} (\xi_1 - V)] \right\} \quad (3.34)$$

where $\exp[(\xi_1 - V)/k_B T] \gg 1$, since V is now negative Eq 3.34 applies for all reverse bias.

Padovani and Stratton^[15] assumed that the contribution of the free electrons to the total space-charge density was negligible. This assumption has been discussed in details by Conley and Mahan^[16] with the conclusion that the simple parabolic potential energy

$$E = \frac{q^2 N_d}{2\epsilon_s} (w-x)^2 \quad (3.35)$$

is adequate for most treatment.

Under those approximations, the constants b_{1F} , c_{1F} and f_{1F} are found to be equal to ^[17]

$$b_{1F} = \frac{\xi_1}{E_{oo}} \{ ((E_b - V + \xi_1)^{1/2} (E_b - V)^{1/2} / \xi_1) - \ln[((E_b - V + \xi_1)^{1/2} - (E_b - V)^{1/2}) / \xi_1^{1/2}] \} \quad (3.36)$$

$$c_{1F} = \frac{1}{E_{oo}} \ln[((E_b - V + \xi_1)^{1/2} + (E_b - V)^{1/2}) / \xi_1^{1/2}] \quad (3.37)$$

$$f_{1F} = \frac{1}{4\xi_1 E_{oo}} (E_b / (E_b + \xi_1))^{1/2} \quad (3.38)$$

where E_{oo} is the constant defined by eq.(3.18), E_b is the barrier-height potential energy ($q\phi_b$), V the applied bias in energy units, and ξ_1 the Fermi energy of the conductor 1. Similarly, in the reverse direction, the coefficients b_{1F} , c_{1F} and f_{1F} can be expressed as

$$b_{2F} = \frac{1}{E_{oo}} \{ ((E_b - V + \xi_1)^{1/2} (E_b)^{1/2} / \xi_1) + (V - \xi_1) \ln[((E_b - V + \xi_1)^{1/2} - (E_b)^{1/2}) / (\xi_1 - V)^{1/2}] \} \quad (3.39)$$

$$c_{2F} = \frac{1}{E_{oo}} \ln[((E_b - V + \xi_1)^{1/2} + (E_b)^{1/2}) / (\xi_1 - V)^{1/2}] \quad (3.40)$$

$$f_{2F} = \frac{1}{4(\xi_1 - V)E_{oo}} ((E_b - V - \xi_1) / (E_b))^{1/2} \quad (3.41)$$

In case of a Schottky barrier the condition in (3.22) can be reduced to

$$k_b T < 2E_{\dots} (\ln[4E_b / \xi_1] + (2E_{\dots} / \xi_1)^{1/2})^{-1} \quad (3.42)$$

As an example, Padovani and Stratton^[15] calculated for Au-n-type GaAs barrier as a function of the semiconductor carrier concentration. Fig.3.7 shows that, the field emission will occur at low temperatures or heavily doped semiconductor. The theory will be compared with results obtained for Au-Si diodes with an impurity concentration of 8×10^{18} atom/cm³. The forward characteristic of such a diode at 77 K is shown Fig.3.8 as can be seen, a linear dependence of the logarithm of the current on the applied bias.

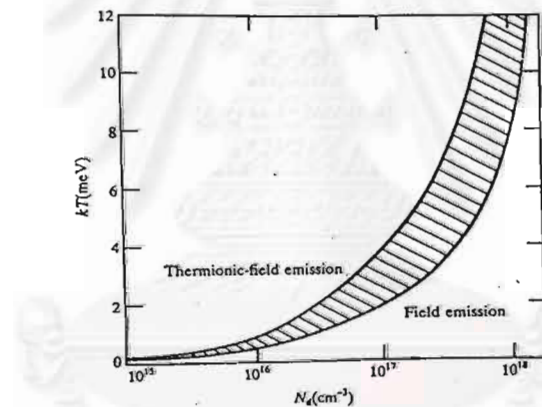


Fig.3.7 N_d versus $k_b T$ for Au- GaAs Schottky barrier as a function of the semiconductor impurity concentration^[17].

The figure gives for a given carrier concentration the range of temperatures where the conduction properties of the barrier are dominated by either T-F or F emission, The cross-hatched region corresponds to temperatures where both conditions do not apply^[17].

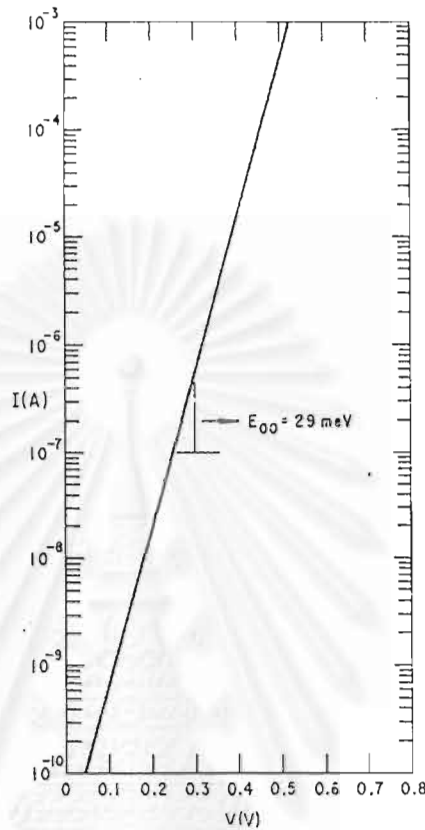


Fig. 3.8 Forward V-I characteristic of a gold heavily doped n-type silicon diode at 77 K^[17].

Therefore, the complex energy-momentum relationship for the tunnel electrons has been assumed to be parabolic. This is certainly not the case for metal-semiconductor junction where the barrier height is an appreciable fraction of the energy gap, as in the case of n-type GaAs junctions, where $\frac{q\phi_b}{E_g} = \frac{2}{3}$. In this case, the electron tunneling in the energy gap has acquired a considerable valence-band character before encountering the metal surface. The electron energy-momentum relationship in the forbidden gap can be

calculated by assuming a two-band model. If the effective mass is small, Franz' experimental expression for kinetic energy,

$$E' = (E_G^2 / 4) + (E_G \frac{p^2}{2m^*})^{1/2} - (E_G / 2), \quad (3.43)$$

can be used. If a more accurate relation is sought, Kane's expression^[18] for the momentum,

$$\frac{p^2}{2m} = \frac{E'(E' + E_G)(E' + E_G + \Delta)(E_G + (2\Delta / 3))}{E_G(E_G + \Delta)(E' + E_G + (2\Delta / 3))} \quad (3.44)$$

where Δ is the value of spin-orbit splitting is used instead. The Franz, parabolic and Kane energy-momentum relationship for GaAs are shown in Fig.3.9.

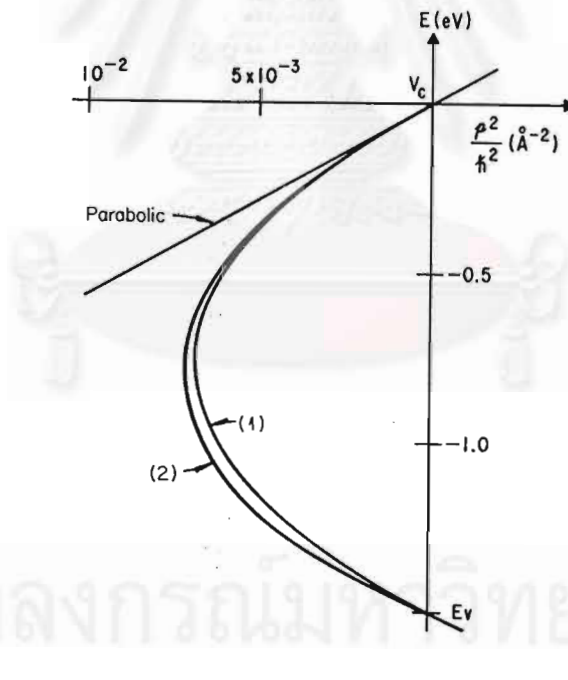


Fig 3.9 The parabolic (1) ,Franz (2) ,and Kane dispersion relationships as computed for GaAs^[17].

The influence of a nonparabolic energy-momentum relation on the V-J characteristic of a tunneling junction was first considered by Padovani and Stratton^[1]. Let consider the case where p_m , the maximum value of the component of the quasi momentum parallel to the plane of the junctions, is large enough that the last integral in eq.(3.21) can be neglected. Let us also assume the Fermi energy of the semiconductor is sufficiently large to satisfy the inequality

$$c_{if} \xi_1 > 1. \quad (3.45)$$

This condition are equivalent to assuming that the major contribution to the tunneling current came from electrons located in the vicinity of the semiconductor Fermi level. It then follows that eq.(3.21) can be expressed as

$$J \propto \exp[-b_{if}] \quad (3.46)$$

In this expression, The constant of proportionality is a slowly varying function of the applied bias. Stratton and Padovani in Ref.[14] have presented a further check of their experimentally deduced energy-momentum relationship by studying the influence of this relationship on the shape of the forward characteristic at low biases (shown in Fig.3.10).

จุฬาลงกรณ์มหาวิทยาลัย

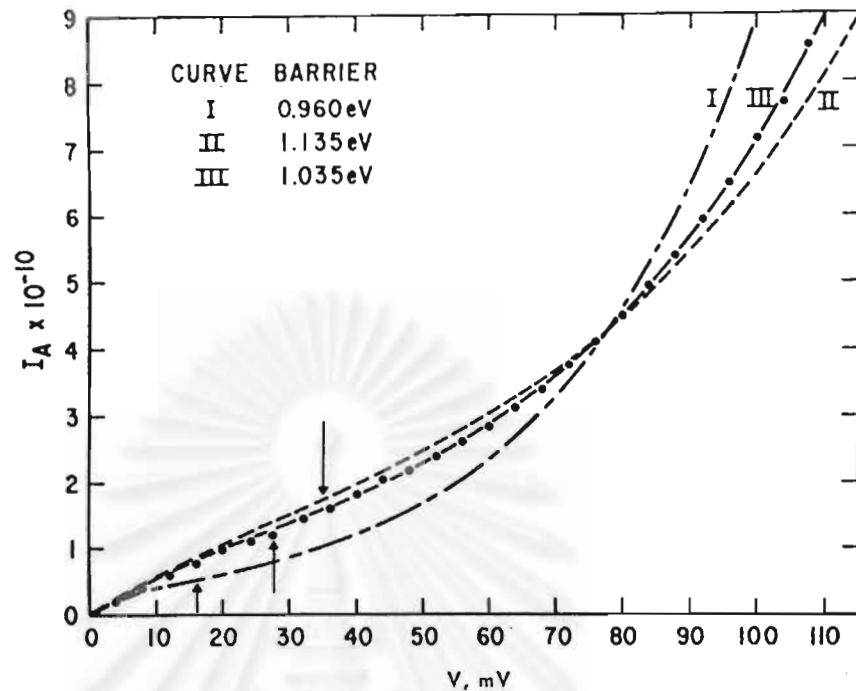


Fig. 3.10 Low bias forward characteristic of a Au-n-type GaAs Schottky barrier. Computed curves by : (I) parabolic bands , (II) Kane's band, (III) experimentally deduced bands dots indicate experimental points and arrows indicate inflection points. Curve barrier : (I) , 0.960 eV ;(II) 1.135 eV, (III), 1.035 eV (From Stratton in reference [14]).

3.3 Contact Resistance

An ohmic contact of a metal-semiconductor contact is defined as a negligible contact resistance relative to the bulk or spreading resistance of the semiconductor. The voltage –current characteristics of Schottky barrier diode and of an ohmic contact are compared in Fig.3.11. Ideally, an ohmic contact has a linear voltage –current characteristic.

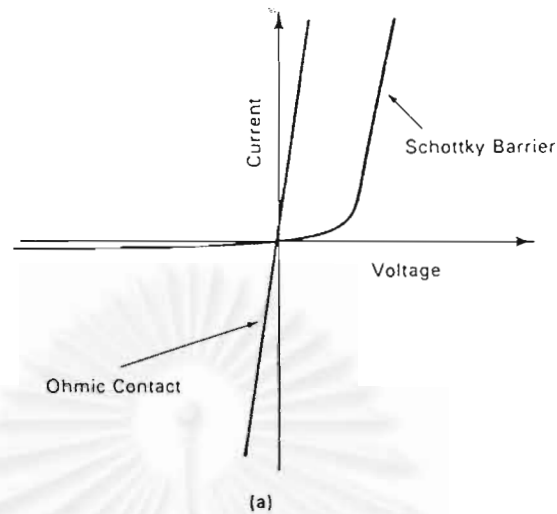


Fig. 3.11 Voltage –current characteristics of Schottky barrier diode and of an ohmic contact ^[13].

An ohmic contact to an n-type semiconductor should also ideally be made using a metal with a lower work function than that of a semiconductor. Unfortunately, very few practical material systems satisfy this condition, and metals usually form Schottky at semiconductor interfaces. Therefore, a practical way to obtain a low resistance ohmic contact is to increase the doping near the metal-semiconductor interface to a very high value so that the depletion layer caused by the Schottky barrier becomes very thin and the current transport through the barrier is enhanced by tunneling (field emission regime; see section 3.2).

Field emission is of considerable importance in connection with ohmic contacts to semiconductors, which usually consist of Schottky barriers on very highly doped semiconductors. The specific differential resistance R_c around zero bias is defined as ^[19]

very highly doped semiconductors. The specific differential resistance R_c around zero bias is defined as^[19]

$$R_c = \left(\frac{\partial J}{\partial V} \right)_{V=0}^{-1} \quad (3.46)$$

For metal-semiconductor contacts with higher doping concentrations, the tunneling process will dominate, and the current density is given by eq. (3.46). Then

$$R_c \propto \frac{\exp[q\phi_b / E_{\infty}]}{E_{\infty}} \quad (3.47)$$

where E_{∞} define by eq.(3.18), theoretical calculations of R_c have been published by Chang , Fang, and Sze^[19] for contacts to silicon an gallium arsenide. The experimental results of R_c for various metals on silicon samples are in good agreement with predictions and shown in Fig. (3.12). In chapter 4, we have presented contact resistance for check of their V-I characteristic at low biases.

สถาบันวิทยบริการ
จุฬาลงกรณ์มหาวิทยาลัย

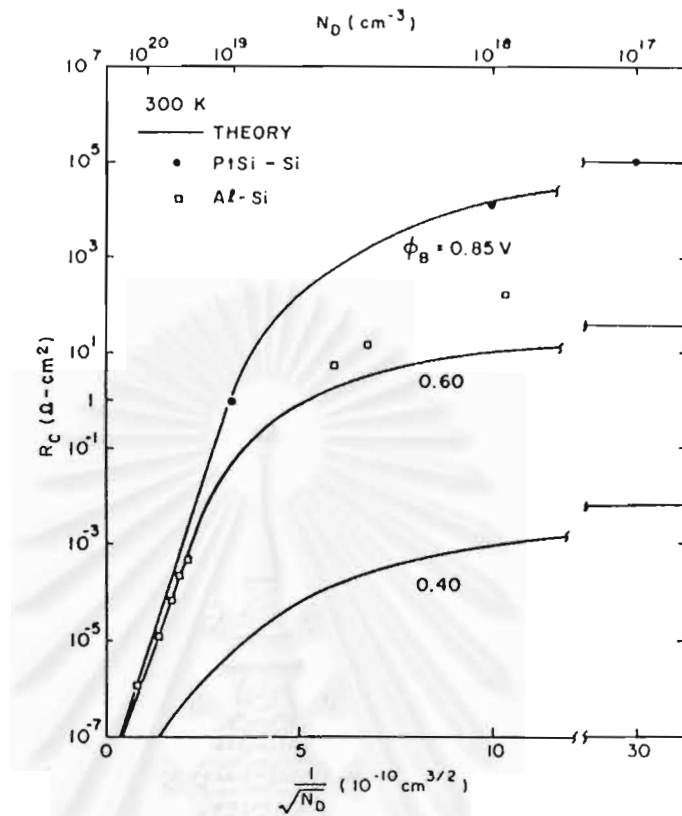


Fig. 3.12 Theoretical (solid lines) and experimental (dots) values of specific contact resistance. ^[19]

จุฬาลงกรณ์มหาวิทยาลัย

Chapter 4

Field Emission for Parabolic Case

In this chapter, we want to know more accurately than the depletion approximation. We must allow for the fact the majority carrier concentration does not fall abruptly to zero but penetrates into the depletion region. The analysis will be developed for an n-type semiconductor.

4.1 Asymptotic Solution of Poisson's Equation

The Schottky barrier assumes that a barrier has been established as described in Fig. 3.1 and assuming the semiconductor to be degenerate, the electron concentration in the depletion region $n(x)$ is given by^[20]

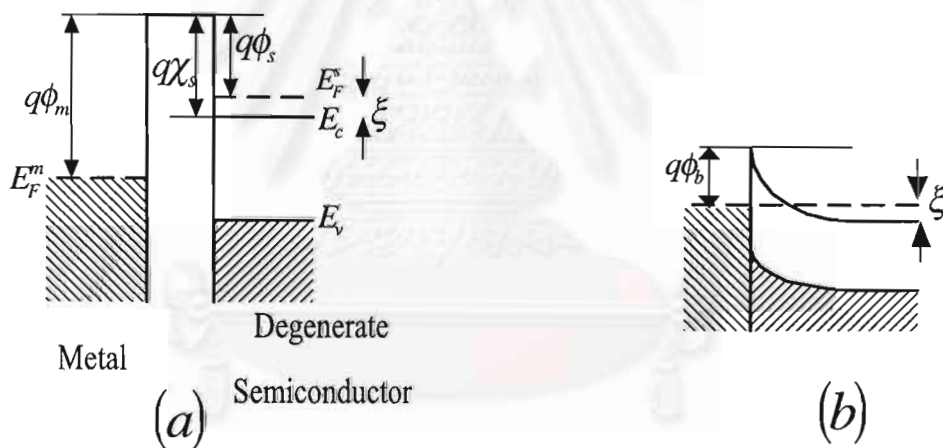


Fig. 4.1 Formation of barrier between a metal and a degenerate semiconductor
(a) neutral and isolated, (b) in perfect contact.

$$n(x) = N_c F_{1/2}((q\phi(x) + \xi)/k_b T) \quad (4.1)$$

where $F_{1/2}(x)$ is the Fermi-Dirac integral (defined by eq.(2.8)), $\phi(x)$ is the electrostatic potential within the semiconductor at a distance x from the interface, k_b is Boltzmann's constant, T is absolute temperature, q is magnitude of electronic charge. The Fermi level $\xi = E_f - E_c$ would be positive for degenerate semiconductors. The conduction band edge in the bulk is taken as the zero potential reference. Thus the sign of the electrostatic potential is negative in the space-charge region.

In the ideal contact, we neglect the surface states. The net charge density is given by

$$\rho(x) = q[N_d - n(x)] \quad (4.2)$$

where N_d is the donor impurity density.

The charge density and electrostatic potential are related by Poisson's equation. It is convenient to introduce new variables $u = \frac{q\phi}{k_b T}$ and $v = \frac{\xi}{k_b T}$. Hence

$$\frac{d^2 u(x)}{dx^2} = \frac{-q^2}{\epsilon_s k_b T} [N_d - N_c F_{1/2}(u(x) + v)]. \quad (4.3)$$

where ϵ_s is the permittivity of the semiconductors. Equation (4.3) is the differential equation for the potential distribution in an arbitrarily doped n-type semiconductor. Unfortunately, this equation cannot be solved in the general case, and approximations must be made to obtain solutions appropriate to specific situations.

To proceed, we consider two special cases. In the first, the Fermi level near the conduction band edge (i.e. $q|\phi|$ is much larger than ξ in the depletion region) we may expand $F_{1/2}(u+v)$ in eq. (4.3) in Taylor's series, and retain only first two terms, which yields

$$\frac{d^2u(x)}{dx^2} \approx -\frac{q^2N_d}{\epsilon_s k_b T} \left[1 - \left(\frac{F_{1/2}(u)}{F_{1/2}(v)} + \frac{F_{-1/2}(u)}{F_{-1/2}(v)} v \right) \right], \quad (4.4)$$

where $N_c F_{1/2}(v) = N_d$. For $|u| \gg v$ and u is negative, the second and third terms in the square bracket in eq. (4.4) are small compared to unity and can thus be neglected

$$\frac{d^2u(x)}{dx^2} = \frac{-q^2N_d}{\epsilon_s k_b T}. \quad (4.5)$$

This result may also be obtained in the simple way by counting only the numbers of positive charges exist on ionized donor atoms. As was discussed in the depletion approximation (section 3.1). The electrostatic potential $\phi(x)$ at x is parabolic given by

$$\phi(x) = -\frac{qN_d}{2\epsilon_s} (w-x)^2, \quad (4.6)$$

where $w^2 = \frac{2\epsilon_s \phi_b}{qN_d}$ (depletion width), ϕ_b is the height of barrier relative to the Fermi level. This approximation is very good for non-degenerate semiconductors (i.e., ξ is negative).

In the opposite limiting case when the Fermi level is much larger than the conduction band edge (i.e. $v \gg |u|$). Thus eq. (4.3) becomes

$$\frac{d^2 u(x)}{dx^2} \approx \frac{q^2 N_d}{\epsilon_s k_B T} \left(\frac{F_{-1/2}(v)}{F_{1/2}(v)} u \right) \quad (4.7)$$

For degenerate semiconductors, $v > 1$, from eq. (2.16) we find the electrostatic potential to be

$$\phi(x) = \phi_b \exp[-\alpha x] \quad (4.8)$$

where $\alpha = \sqrt{\frac{3q^2 N_d}{2\epsilon_s \xi}}$ and $\xi = k_B T \left(\frac{3\sqrt{\pi} N_d}{4N_c} \right)$

In this case, the majority carrier concentration does not fall abruptly to zero, but penetrates into the depletion region and cannot be neglected compared to the donor concentration. Eq. (4.8) is applicable to highly degenerate semiconductors.

In the general case, the parabolic solution valid near the top of Schottky barriers, where $n(x)$ is very small compared to N_d , and the exponential solutions valid near the bottom of Schottky barriers, where $n(x)$ approaches N_d . The electrostatic potential of an M-S junction can be approximated by an exponential barrier shape that provided in eq. (4.8) (shown in Fig. 4.2).

The contact potential $q\phi_b$ in eq. (4.6) and eq. (4.8) is linearly dependent on the work function of metal. The contact potential for GaAs with various metals is shown in Table 4.1, where the positive and negative contact potential is rectifying or Ohmic, respectively.

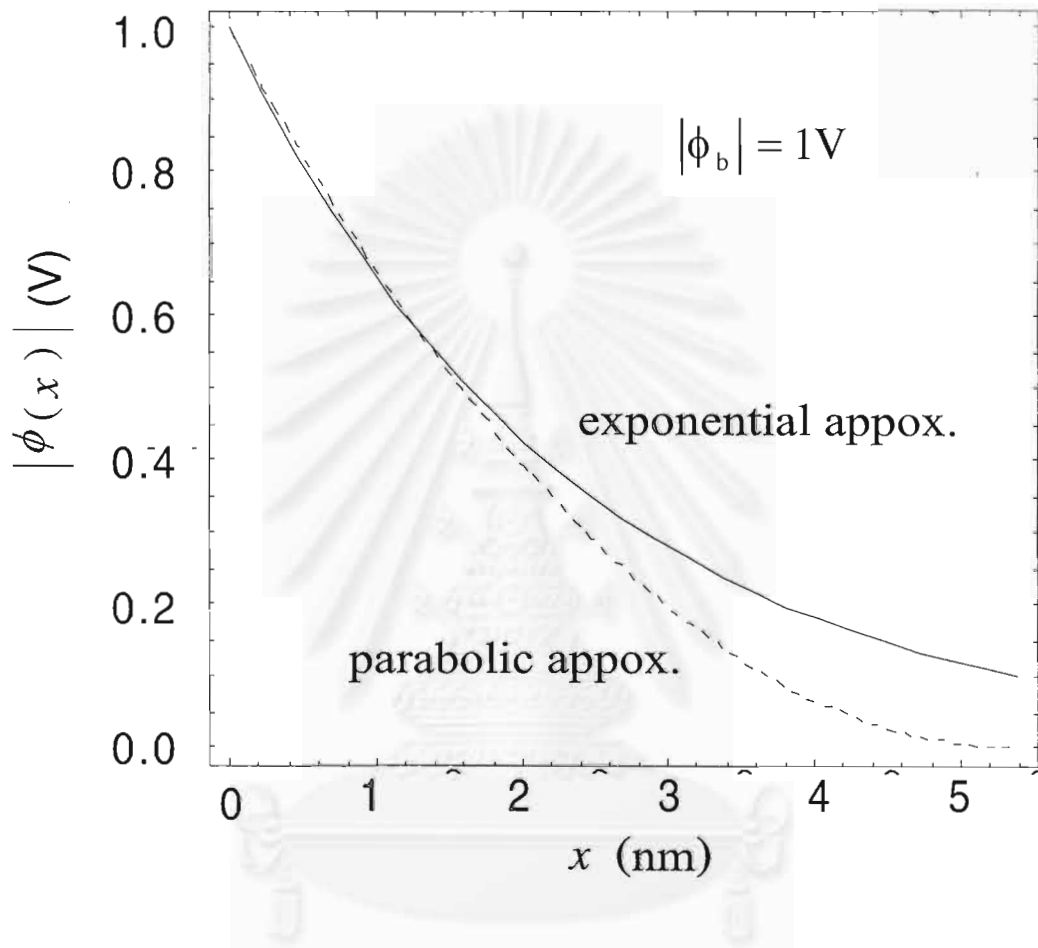


Fig.4.2 Parabolic and exponential potentials for an Au-GaAs junction (GaAs with $N_d = 5 \times 10^{19}$ atoms/cm³ at 243 K).

Metal	Work function (eV)	Contact potential ($q\phi_b$) (eV)
Pt	5.65	1.63
Ni	5.15	1.08
Pd	5.12	1.05
Au	5.10	1.03
Co	5.00	0.93
Cu	4.65	0.58
Mo	4.60	0.53
W	4.55	0.48
Fe	4.50	0.43
Cr	4.50	0.43
Sn	4.42	0.35
Ti	4.33	0.26
Al	4.28	0.21
Ag	4.26	0.19
Ta	4.25	0.18
Ga	4.20	0.13
In	4.12	0.05
Mg	3.66	-0.48
Ca	2.87	-1.2
Ba	2.70	-1.37
Cs	2.14	-1.93

Table 4.1 Work functions and contact potentials for some common metals contacted with GaAs of which electron affinity equal to 4.07 (V)^[2].

4.2 The V-I characteristics

In degenerate semiconductors, especially in semiconductors with small electron effective mass such as GaAs, electrons can tunnel through the barrier near the Fermi level and the tunneling current is dominant. Such a mechanism is called field emission. The current-voltage characteristic is determined by the coefficients b_{1F}, c_{1F} and f_{1F} defined by eqs. (3.24), (3.25) and (3.26), respectively. These quantities are dependent on the Schottky barrier shape. Under the depletion approximation, Padovani and Stratton^[15] have given the values of b_{1F}, c_{1F} and f_{1F} in eqs. (3.36), (3.37) and (3.38), respectively. This has been discussed in section 3.2. At arbitrary doping and under the condition

$$\xi = \phi_b \exp \left[-\alpha \left(w - \sqrt{\frac{2\epsilon_s \xi}{q^2 N_d}} \right) \right] \quad (4.9)$$

where $\xi = k_b T \left[\frac{3\sqrt{\pi} N_d}{4N_c} \right]^{2/3}$ and w is the depletion width in parabolic barrier. In Fig. 4.3, the condition (4.9) was calculated for Au-GaAs Schottky barrier as a function of the donor concentration. We obtain the temperatures operation for the electrostatic potential of an M-S junction can be approximated by an exponential barrier shape that provided in eq. (4.8). The figure gives the relationship of donor concentration and temperatures where the potential of junction can be approximated by an exponential barrier.

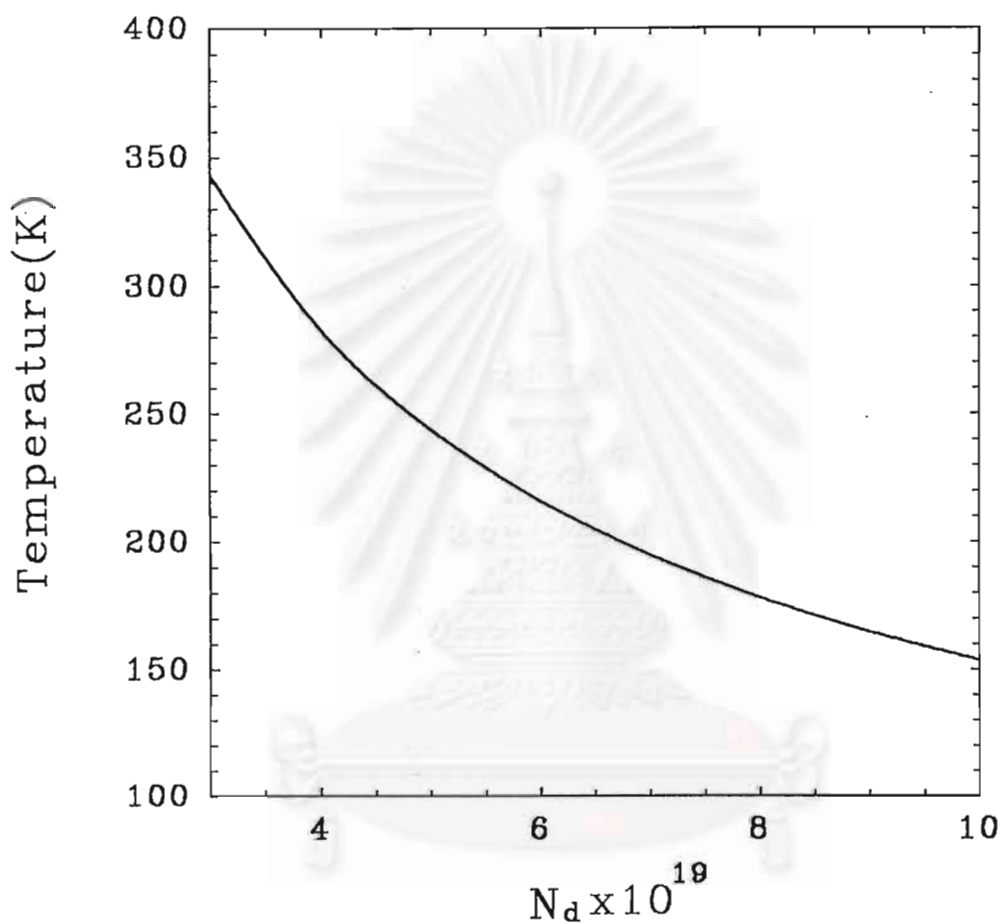


Fig.4.3 The relationship of donor concentration. (atoms/cm³) and temperatures calculated for Au-GaAs Schottky barrier.

The bottom of conduction band (defined by eq. (3.5)) is given by

$$E_c(x) = E_b \exp[-\alpha x], \quad (4.10)$$

where E_b is the contact potential energy. Neglecting the image force at low bias for simplicity. The quantity b_{1F} in eq. (3.24) can be expressed as

$$b_{1F} = \frac{2}{\hbar} \int_0^{E_b-V} \frac{(\bar{p})_\xi}{(d\eta/dx)} d\eta. \quad (4.11)$$

If V is the applied voltage, the energy of electrons in the barrier is given by

$$\eta(x) = E_b \exp[-\alpha x] - \xi \quad (4.12)$$

Substituting eq. (4.11) in eq. (4.10) gives

$$b_{1F} = \frac{4\sqrt{\xi}}{3E_{\infty}} \left[\sqrt{E_b - V} - \sqrt{\xi} \tan^{-1} \sqrt{\frac{E_b - V}{\xi}} \right], \quad (4.13)$$

where E_{∞} is defined by eq. (3.18).

Similarly, the coefficients c_{1F} and f_{1F} can be expressed as

$$c_{1F} = \frac{2}{\sqrt{3}E_{\infty}} \tan^{-1} \sqrt{\frac{E_b - V}{\xi}}, \quad (4.14)$$

$$f_{1F} = \frac{1}{2\sqrt{3}E_{\infty}} \left[\frac{1}{\sqrt{\xi(E_b - V)}} + \frac{1}{\xi} \tan^{-1} \sqrt{\frac{E_b - V}{\xi}} \right] \quad (4.15)$$

For parabolic relationship between energy and momentum in the conductor and the insulator (depletion region), eq. (3.21) then reduces to eq. (3.32), (3.33) and (3.34). The expression for the V-I characteristic can now be obtained by

replacing the coefficients b_{1F} and c_{1F} in eq. (3.32) and eq. (3.33). In the reverse direction, the coefficients b_{2F} , c_{2F} and f_{2F} can be expressed as

$$b_{2F} = \frac{4}{3E_{..}} \left[\sqrt{E_b(\xi - V)} - (\xi - V) \tan^{-1} \sqrt{\frac{E_b}{\xi - V}} \right], \quad (4.16)$$

$$c_{2F} = \frac{2}{\sqrt{3}E_{..}} \tan^{-1} \sqrt{\frac{E_b}{\xi - V}}, \quad (4.17)$$

$$f_{2F} = \frac{1}{4\sqrt{3}E_{..}} \left[\frac{1}{\sqrt{E_b(\xi - V)}} + \frac{1}{\xi - V} \tan^{-1} \sqrt{\frac{E_b}{\xi - V}} \right]. \quad (4.18)$$

The validity of these results is subjected to the condition in (3.22). Since a Schottky barrier presents the largest depletion layer for tunneling at zero bias, one can be sure that the field emission exists at all biases provided that condition is fulfilled at zero bias. It can be shown that in the case of a exponential Schottky barrier this condition implies that the temperature is such that

$$\left[\frac{2}{\sqrt{3}E_{..}} \tan^{-1} \sqrt{\frac{E_b}{\xi}} + \left(\frac{1}{2\sqrt{3}E_{..}} \left[\frac{1}{\sqrt{E_b(\xi)}} + \frac{1}{\xi} \tan^{-1} \sqrt{\frac{E_b}{\xi}} \right] \right)^{1/2} \right]^{-1} - k_b T > 0, \quad (4.19)$$

the tunneling current is dominant.

As an example, the condition (4.19) was calculated for the Au – GaAs (n – type) barrier as a function of the semiconductor carrier concentration. Fig. 4.4 shows that, for reasonable carrier concentrations, field emission will only occur at low temperatures.

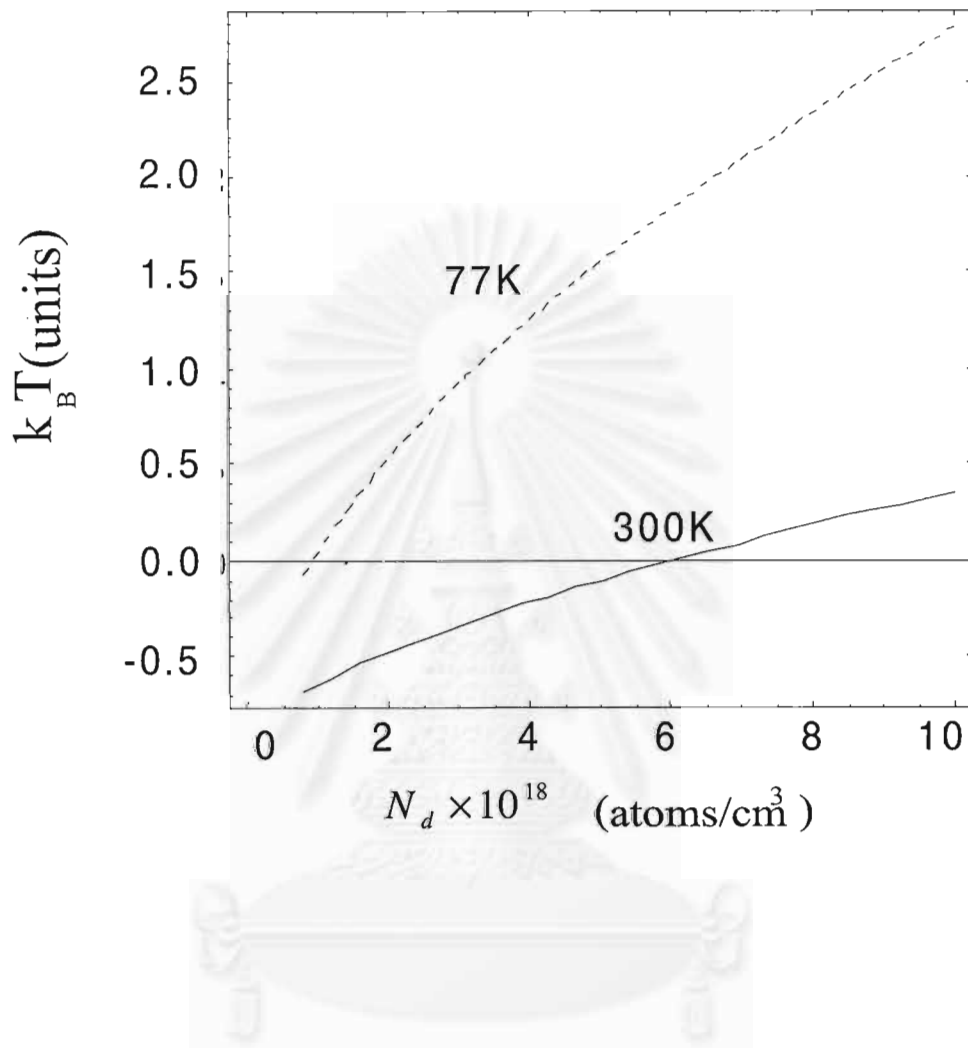
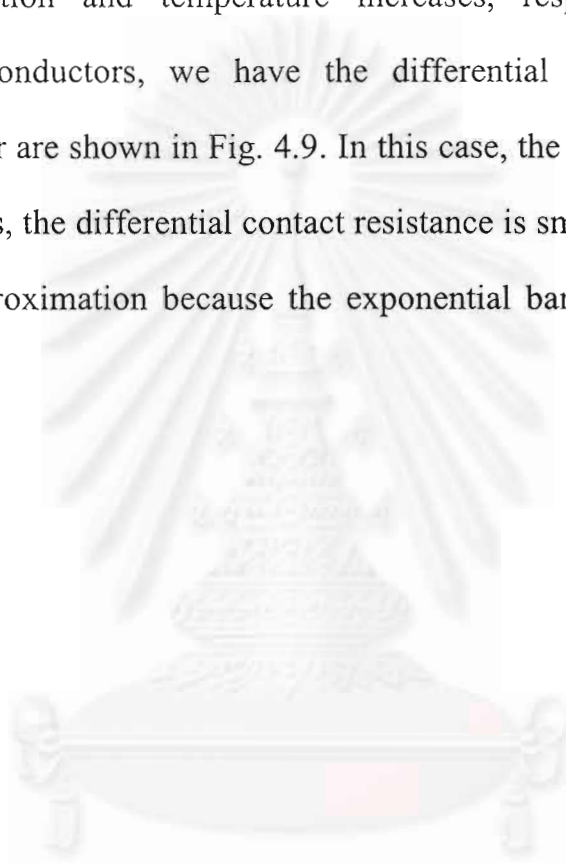
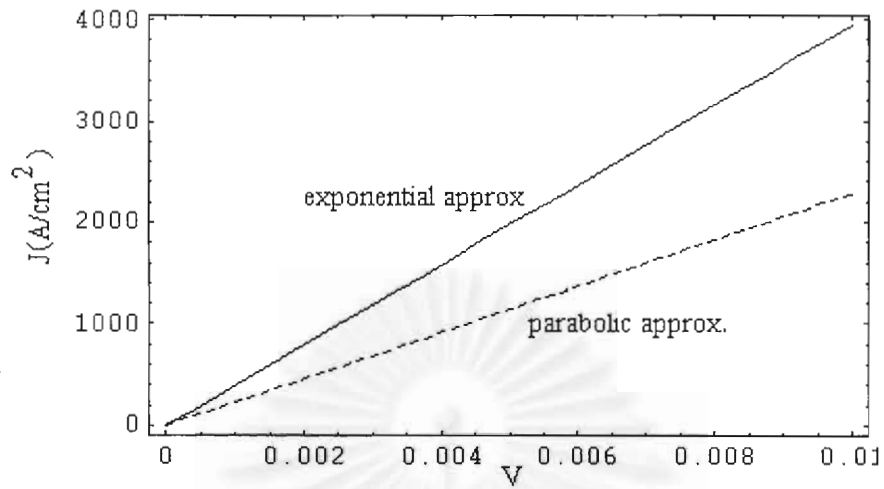


Fig. 4.4 The relationship (condition (4.19) in thermal energy ($k_b T$) units) of donor concentration and temperatures calculated for Au-GaAs Schottky barrier at 300K and 77K.

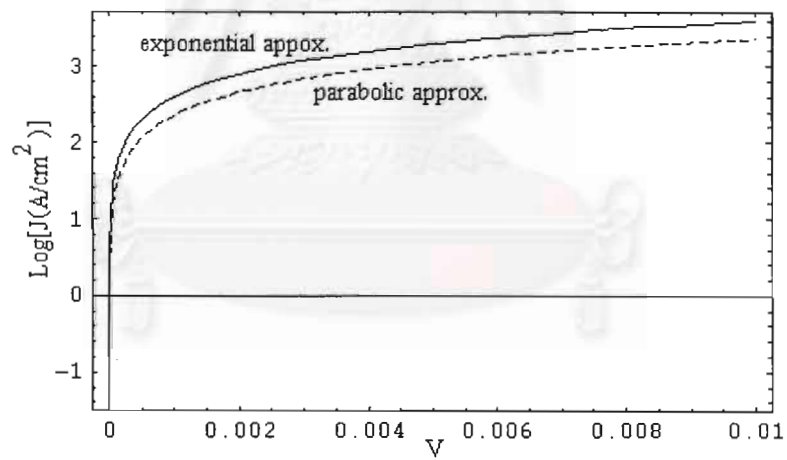
The voltage–current characteristics at low bias for an Au–GaAs diode with the parabolic and the exponential approximations of Schottky barrier shapes shown in Fig. 4.5. In Figs. 4.6, 4.7 and 4.8, show that, the tunneling current density in metal–semiconductor contact increases if the contact barrier decreases, or if the doping concentration and temperature increases, respectively. For highly degenerate semiconductors, we have the differential resistance R_c of the exponential barrier are shown in Fig. 4.9. In this case, the majority carrier cannot be neglected. Thus, the differential contact resistance is smaller than predicted by the depletion approximation because the exponential barrier approached to the exact barrier.



สถาบันวิทยบริการ
จุฬาลงกรณ์มหาวิทยาลัย



(a)



(b)

Fig.4.5 The voltage–current characteristics for an Au–GaAs ($N_d = 1 \times 10^{19}$ atoms/cm³) diode at 77K with the parabolic and the exponential approximations of Schottky barrier shapes in the normal scale (a) and the log scale (b).

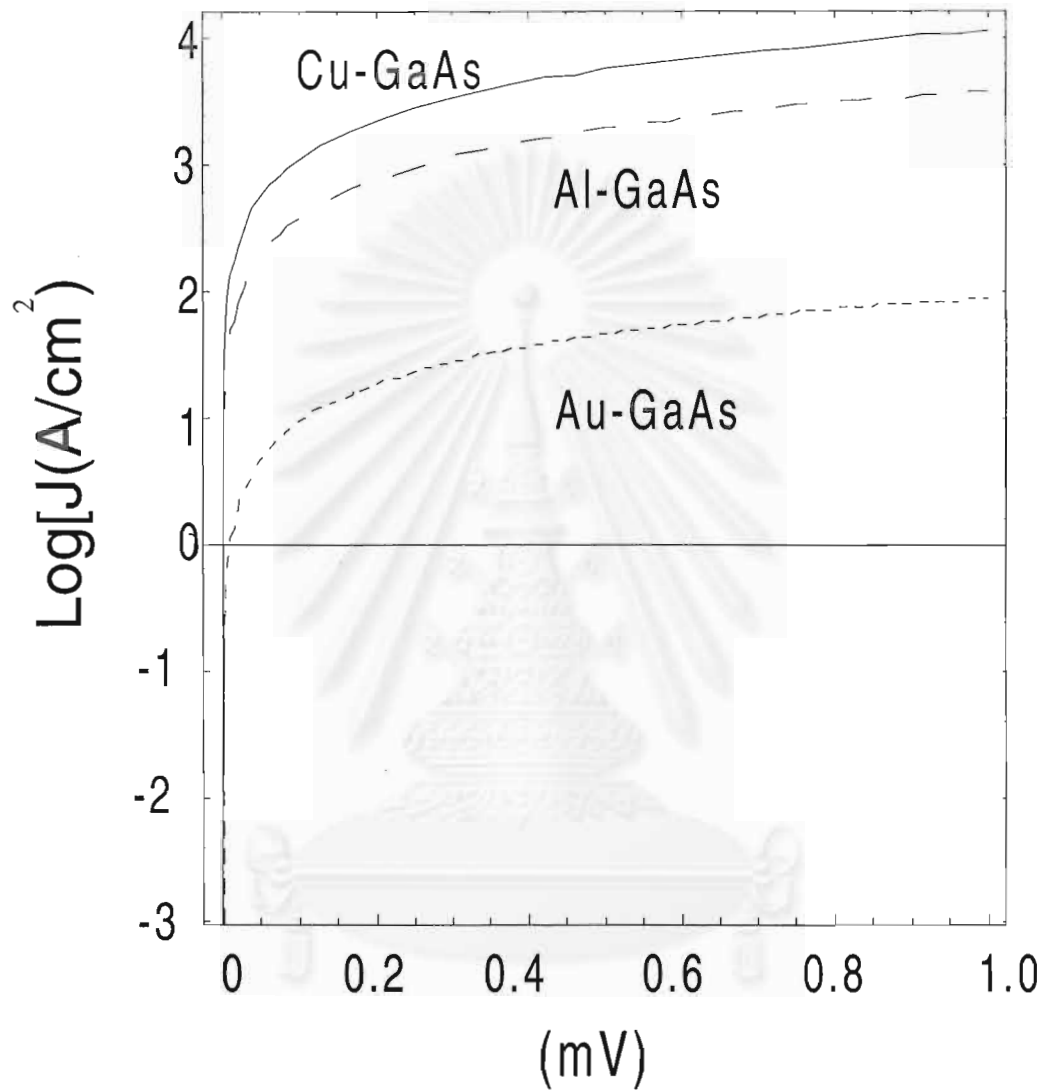


Fig.4.6 The voltage–current characteristics for Au-GaAs, Al-GaAs, and Cu-GaAs diode ($N_d = 5 \times 10^{19} \text{ atoms}/\text{cm}^3$) at 77 K.

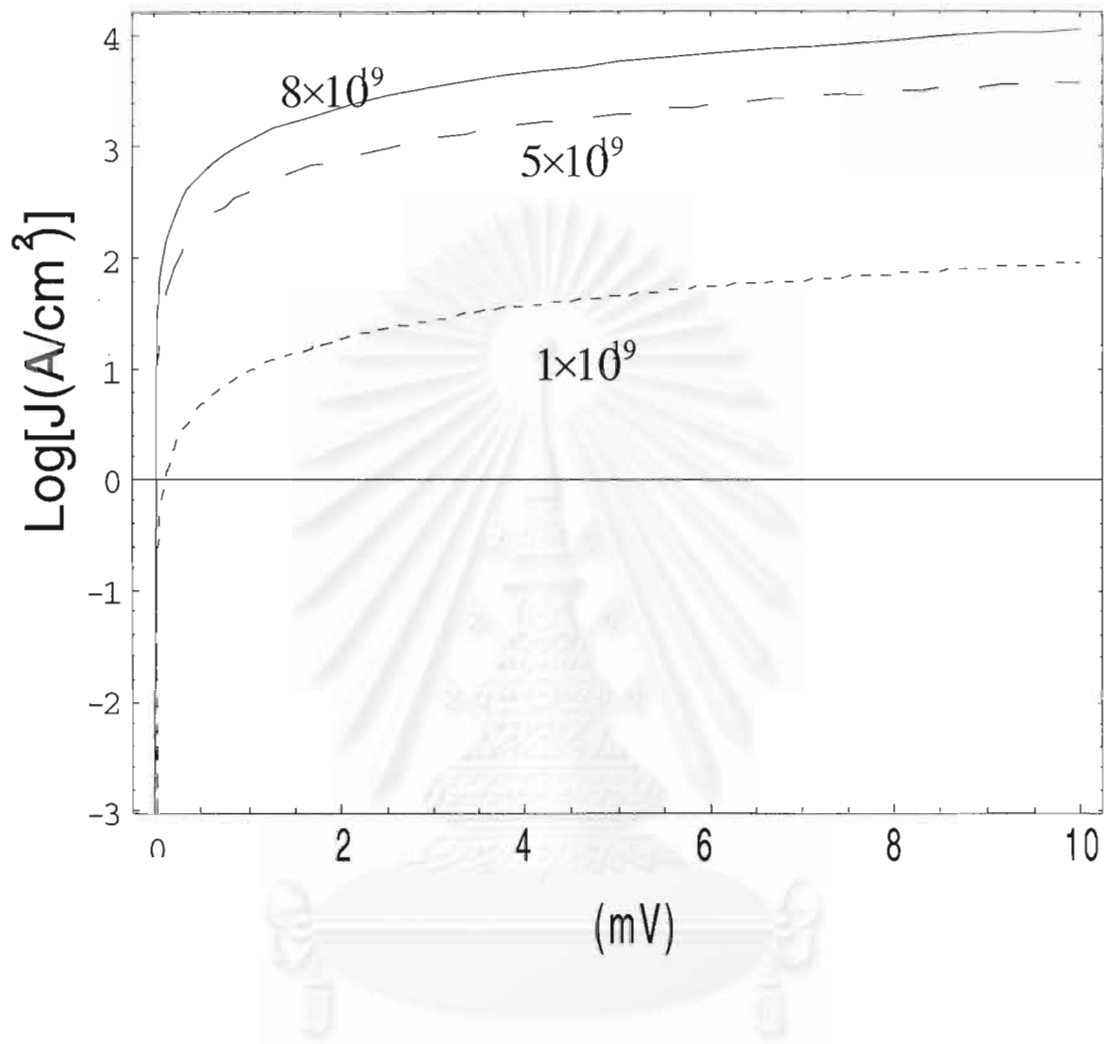


Fig.4.7 The voltage–current characteristic for an Au-GaAs diode for various doping concentration N_d (donors/cm³) at 77 K.

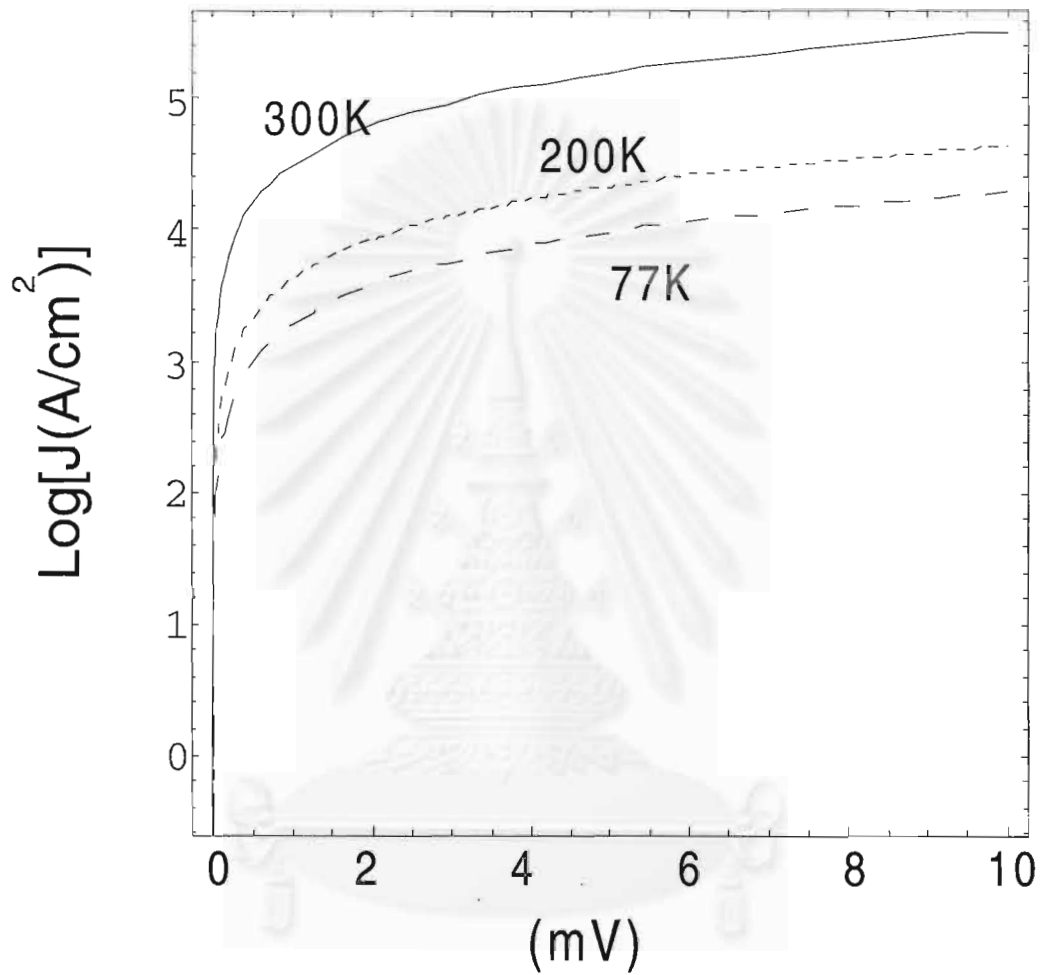


Fig.4.8 The voltage–current characteristic for an Au-GaAs diode ($N_d = 1 \times 10^{20}$ atoms/cm³) at various temperature.

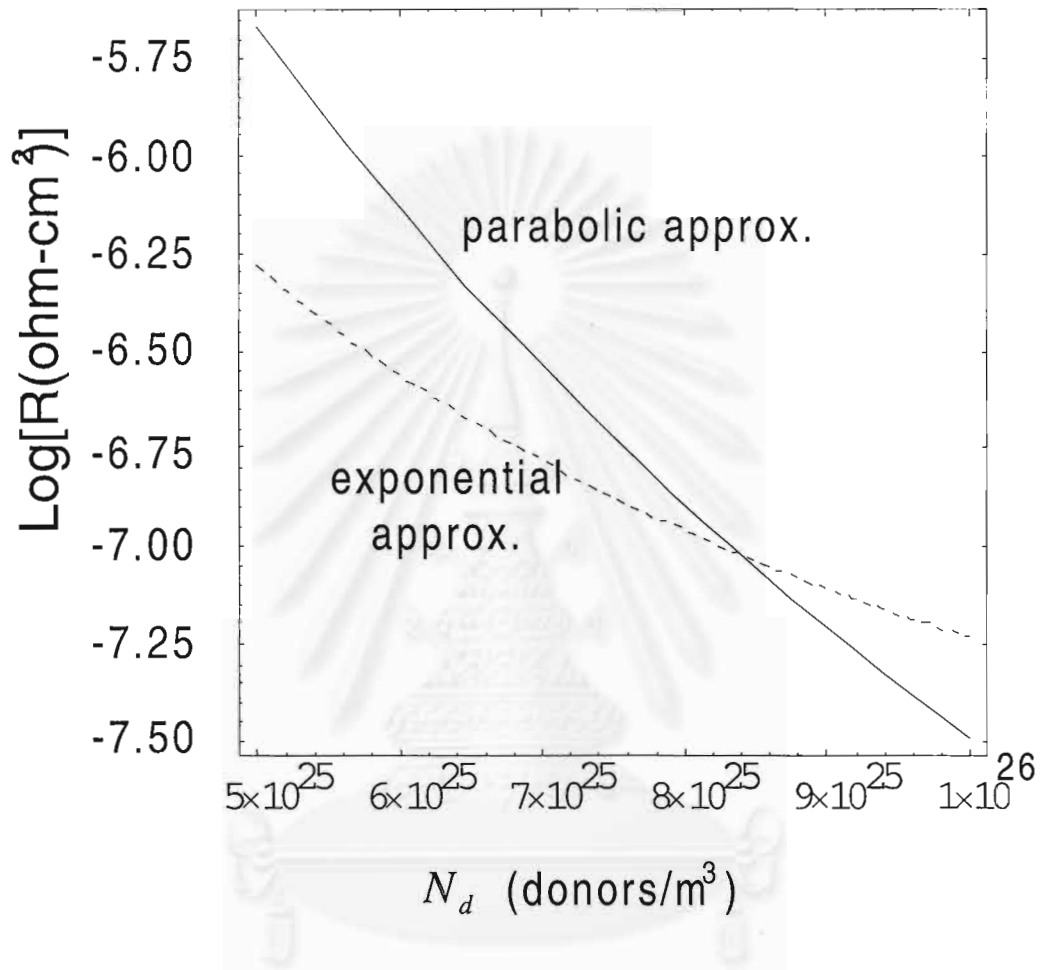


Fig. 4.9 The contact resistance of Au –GaAs in parabolic and exponential barrier approximations at 300K.

Chapter 5

Field Emission of Nonparabolic Case

The influence of the shape of potential barrier on V-I characteristic was considered in previous chapter. In this chapter we consider the influence of a non-parabolic energy-momentum relationship on the V-I characteristic of a Schottky barrier and compare the localized electron transmission probability with the delocalized electron transmission probability in the last section.

5.1 The V-I Characteristic Curve

The effect of nonparabolic energy bands of a potential barrier on tunneling electrons has been previously considered. Stratton and Padovani^[1] have shown that it would lead to an increase of the tunnel current if the barrier height were an appreciable fraction of the forbidden energy gap of the insulator. They have adapted a technique to evaluate the band structure in the forbidden gap of the insulator from the study of the voltage-current characteristic of a tunneling metal-insulator-metal sandwich to the case of a tunneling Schottky barrier and have obtained an experiment determination of part of the complex energy- momentum relationship for GaAs. In this section, we will apply a technique to evaluate the energy-quasi momentum relationship in the forbidden gap of heavily doped semiconductors using the density of states^[5,21,24] and show the V-I characteristic of Schottky barrier.

The total number of states is assumed to be confined within a sphere in \vec{k} space, the integration of density of states function, $\rho(E)$, over the electron energy can yield the following expression

$$k(E) = \left[3\pi^2 \int_{-\infty}^E \rho(E') dE' \right]^{1/3} \quad (5.1)$$

From Kane's Theory, the density of states function is given by

$$\rho(E) = \frac{m^{*3/2}}{4\pi^2 \hbar^3} \xi_Q^{1/4} \exp\left[\frac{-(E-E_c)^2}{4\xi_Q}\right] D_{-3/2}\left(-\frac{(E-E_c)}{\sqrt{\xi_Q}}\right), \quad (5.2)$$

where ξ_Q is the potential fluctuation defined by eq. (2.26) and $D_\nu(x)$ is the parabolic cylinder function. Substituting eq. (5.2) in eq. (5.1) gives

$$k^3(E) = \frac{3m^{*3/2} \xi_Q^{3/4}}{2\hbar^3} \left[\int_{-\infty}^w \exp\left[\frac{-w'^2}{4}\right] D_{-3/2}(-w') dw' \right] \quad (5.3)$$

where $w' = \frac{E-E'}{\sqrt{\xi_Q}}$ and $w = \frac{E-E_c}{\sqrt{\xi_Q}}$.

From Gradshteyn and Ryzhik ^[21] we have

$$\int_{-\infty}^0 \exp\left[\frac{-x^2}{4}\right] D_{-3/2}(-x) dx = \frac{\pi^{1/2}}{2^{5/4} \Gamma(7/4)} \quad (5.4)$$

and

$$\int_0^u \text{Exp}\left[\frac{-x^2}{4}\right] D_{-3/2}(-x) dx = -\frac{\pi^{3/2} \exp[-x^2/4]}{3 \times 2^{21/4} \Gamma(3/4)} (64 \exp[-x^2/4] + G(x)) - \frac{\sqrt{\pi} \exp[-x^2/4]}{2^{37/4} \Gamma(5/4)} (3I_{-3/4}[x^2/4] + 2I_{1/4}[x^2/4] - I_{5/4}[x^2/4]) \quad (5.5)$$

where $G(x) = 5 \times 2^{1/4} \Gamma(-5/4) (I_{-5/4}[x^2/4] - 2I_{-1/4}[x^2/4] - 3I_{3/4}[x^2/4])$,

$I_\nu[x]$ is the modified Bessel function and $\Gamma(n)$ is the Gamma function. Rewrite eq. (5.3) in terms of eq. (5.4) and eq. (5.5) to be

$$k^3(E) = \frac{3m^{*3/2}\xi_Q^{3/4}}{2\hbar^3} \left[\frac{\pi^{1/2}}{2^{5/4}\Gamma(7/4)} + f(w) \right] \quad (5.6)$$

where

$$f(w) = -\frac{\pi^{3/2} \exp[-w^2/4]}{3 \times 2^{21/4} \Gamma(3/4)} (64 \exp[-w^2/4] + G(w)) - \frac{\sqrt{\pi} \exp[-w^2/4]}{2^{37/4} \Gamma(5/4)} (3I_{-3/4}[w^2/4] + 2I_{1/4}[w^2/4] - I_{5/4}[w^2/4])$$

$$\text{and } G(w) = 5 \times 2^{1/4} \Gamma(-5/4) (I_{-5/4}[w^2/4] - 2I_{-1/4}[w^2/4] - 3I_{3/4}[w^2/4]).$$

The quasi momentum ^[24] (p) is defined by $p = \hbar k$, where k is parameter to calculate the tunneling current. Rewriting eq. (5.6) in terms of momentum, we obtain the expression

$$\frac{p^2}{2m^*} = \left[\frac{3\pi^{1/2}\xi_Q^{3/4}}{2^4\Gamma(7/4)} + \frac{3\xi_Q^{3/4}}{2\sqrt{2}} f(w) \right]^{2/3}. \quad (5.7)$$

In view of eq.(5.7), Kane's semiclassical model is used to find the energy – quasi momentum dispersion relation for band tailing (in the forbidden gap of heavily doped semiconductors) where a parabolic dispersion is assumed in the absence of impurities. Since the quasi momentum in Fig.5.1 is an important parameter when the problem associated with the effects of impurity band on the tunneling current, we will then concentrate on the calculation of a relationship between energy and momentum. Assuming the WKB approximation is applicable, the magnitude of complex momentum in parabolic band is replaced by the magnitude of quasi momentum in eq. (5.7) to calculate the transmission coefficient.

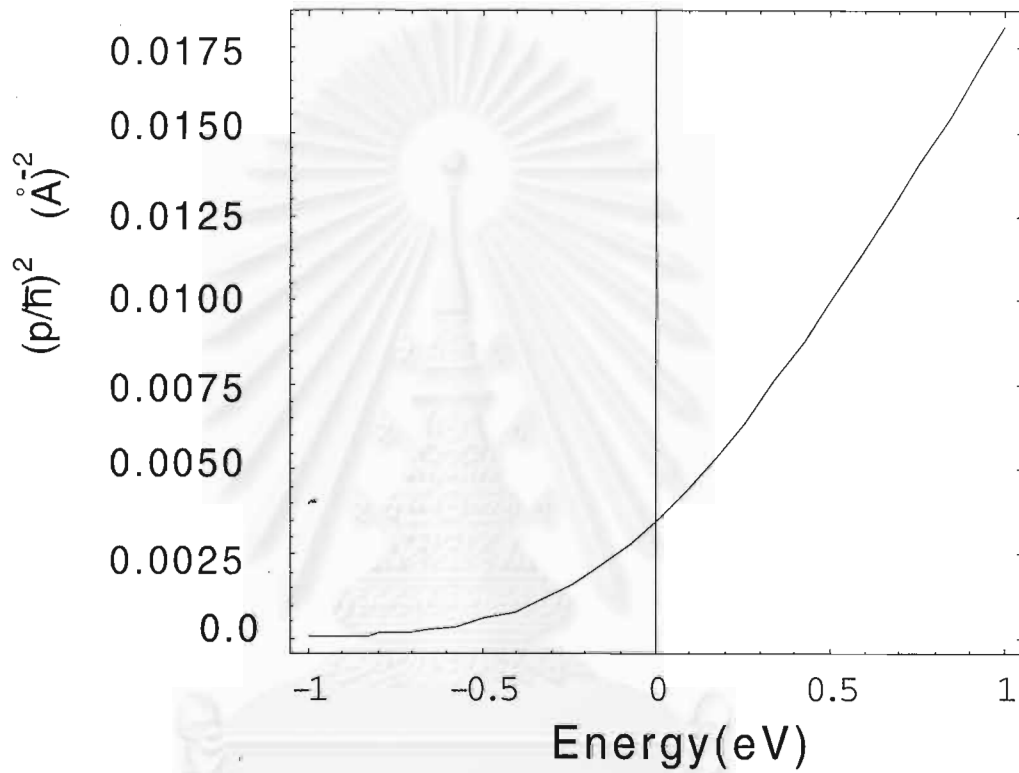


Fig. 5.1 The quasi momentum (eq. (4.7)) computed for GaAs(2×10^{19} donor atoms/cm³).

The tunnel current through an arbitrary potential barrier with arbitrary energy-momentum relationship can be expressed as eq. (3.21). For simplicity, so that the last integral in eq. (3.21) can be neglected with respect to 2π and that the Fermi energy of the semiconductor (ξ_{FS}) is sufficiently large to satisfy the inequality

$$\xi_s / k_B T > c_{1F} \xi_s \gg 1 \quad (5.8)$$

where ξ_s is the Fermi level in semiconductors. Finally, neglecting the energy dependence of the factor p_{01F}^2 with respect to that exponential factor, eq. (3.21) reduces to^[1]

$$J = \frac{2\pi^2 q k_B T p_{01F}^2 \exp[-b_{1F}]}{h^3 \sin(\pi c_{1F} k_B T)} (1 - \exp[c_{1F} V]) . \quad (5.9)$$

The coefficients p_{01F}^2 , b_{1F} , c_{1F} and f_{1F} arise in the Taylor expansion of the logarithm of the transmission coefficient around the Fermi level of semiconductor and are given by eq. (3.23) to (3.26) respectively.

For nonparabolic energy-momentum relationship in the energy gap of semiconductors (eq. 5.7),

$$p(E) = \left(c_1 + c_2 f\left(\frac{E_c - E}{\sqrt{\xi_Q}}\right) \right)^{1/3} \quad (5.10)$$

where $c_1 = \frac{3m^{*1/2}\xi_Q^{1/4}}{2} \left(\frac{\pi^{1/2}}{2^{5/2}\Gamma(7/4)} \right)$ and $c_2 = \frac{3m^{*1/2}\xi_Q^{1/4}}{2}$.

In lightly degenerate semiconductors, the contribution of the free electrons to the total space-charge density was negligible (section 4.1). We can write the parabolic potential energy as eq. (3.35). The constant b_{1F} is given by eq.(3.24). Then, substituting for the momentum from eq.(5.10). This can be rewritten as

$$b_{1F} = \frac{\xi_Q^{1/4}}{\sqrt{2m^* E_{\infty}}} \int_0^{\frac{E_b-V}{\sqrt{\xi_q}}} \frac{(c_1 + c_2 f(\eta(x)))^{1/3}}{\left(\eta(x) + \frac{\xi_s}{\sqrt{\xi_Q}}\right)^{1/2}} d\eta \quad (5.11)$$

where $\eta(x) = \frac{\phi(x) - \xi_s}{\sqrt{\xi_Q}}$ is energy of the electron in the barrier and $\phi(x)$ is the simple parabolic potential energy . Similarly,

$$c_{1F} = \frac{1}{3\sqrt{2m^* E_{\infty} \xi_Q^{1/4}}} \int_0^{\frac{E_b-V}{\sqrt{\xi_q}}} \frac{c_2 f'(\eta)}{\left(\eta(x) + \frac{\xi_s}{\sqrt{\xi_Q}}\right)^{1/2} (c_1 + c_2 f(\eta(x)))^{2/3}} d\eta \quad (5.12)$$

and

$$p_{01F}^2 = \left[\frac{\xi_Q^{1/4}}{\sqrt{2m^* E_{\infty}}} \int_0^{\frac{E_b-V}{\sqrt{\xi_q}}} \frac{d\eta}{\left(\eta(x) + \frac{\xi_s}{\sqrt{\xi_Q}}\right)^{1/2} (c_1 + c_2 f(\eta(x)))^{1/3}} \right]^{-1} \quad (5.13)$$

The coefficients b_{1F}, c_{1F} and p_{01F}^2 is going to result in much more complex. We can obtain numerically this coefficients and the V-I characteristic. The Mathematica program is employed to calculate the V-I characteristic and the result is shown in Fig. 5.2.

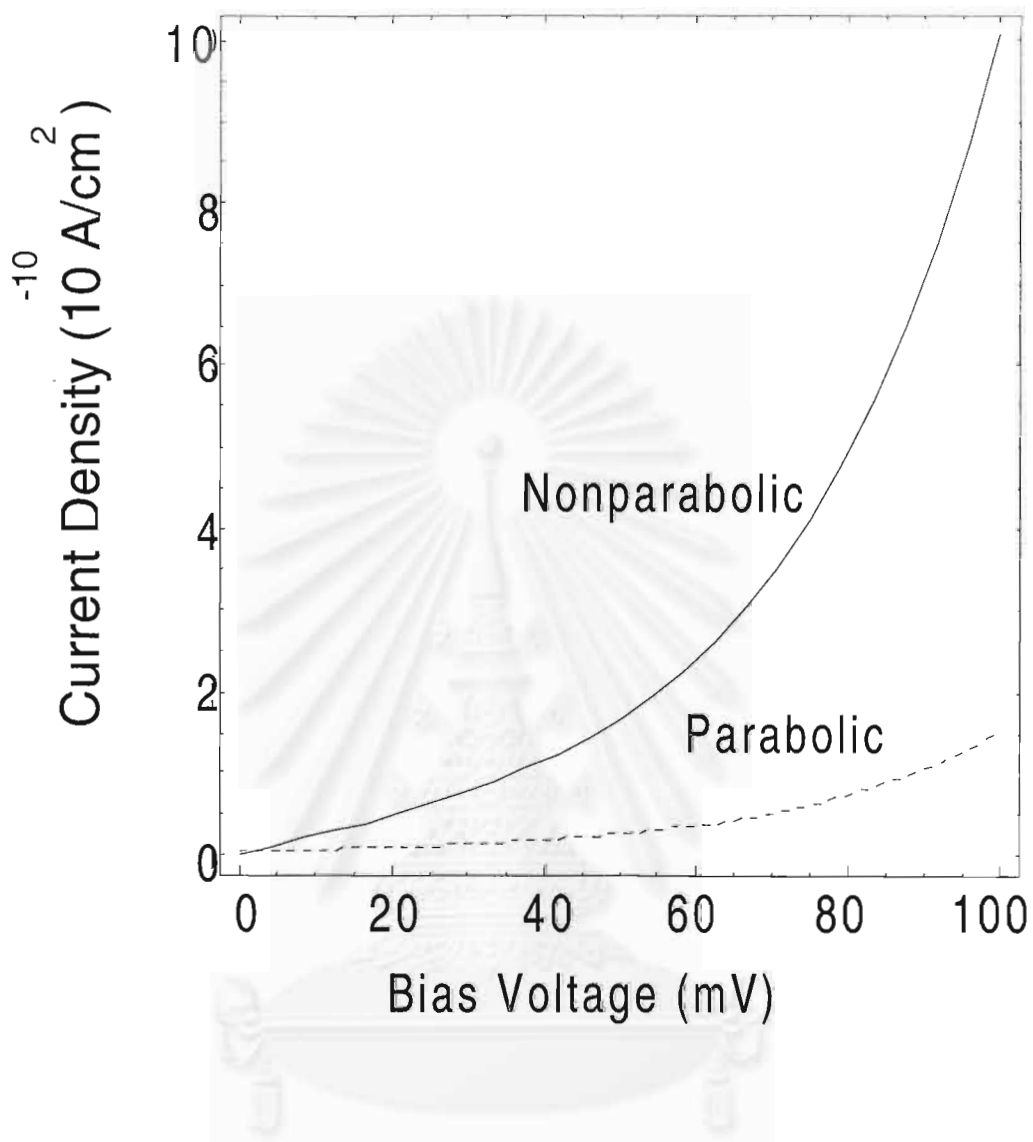


Fig 5.2 The voltage-current characteristic for Au-GaAs diode (2×10^{18} donor atoms/cm³) at 77 K for the parabolic and nonparabolic in eq. (5.10) momentum-energy relationship.

5.1 The Localized Electron Tunneling

The tunneling current in Schottky barrier is proportional to the quantum transmission coefficient multiplied by the occupation probability and the unoccupied probability in the other side. In that way, the tunneling current from the localized states and the delocalized states in the conduction band is different at the quantum transmission coefficient, where the density of states function is applied to any energy of electron. In this section, we consider the quantum transmission coefficient of localized electrons and compare with the transmission coefficient of delocalized electron in the conduction band.

Since Sayakanit and Glyde's density of states (SG's DOS) ^[8] is obtained by using harmonic wells and the model provides Gaussian wave functions. The envelope function for the conduction bands is ^[5]

$$\psi_c(\vec{k}_c, \vec{r}) = \left(\frac{2\alpha_c}{\pi} \right)^{3/4} \exp[i\vec{k}_c \cdot \vec{r}] \exp[-\alpha_c |\vec{r} - \vec{r}_j|^2] \quad (5.14)$$

where the localization parameter (α_c) is related to the variational parameter (z_c) by eq.(2.29) and eq.(2.30). Let us consider the Schottky potential barrier of which the localized electrons in the degenerate semiconductors incident to the potential and penetrate to the metal in other side. We use the wave function of an electron in the conduction band as given by eq. (5.14) which can be rewritten in the form

$$\psi_1(\vec{k}_c, \vec{r}) = g(\vec{r}, k_{cy}, k_{cz}) a_1 \exp[ik_1 x] + g(\vec{r}, k_{cy}, k_{cz}) b_1 \exp[-ik_1 x] \quad (5.15)$$

where $k_1 = k_{cx}$ and

$$g(\vec{r}, \vec{k}_{cy}, \vec{k}_{cz}) = \left(\frac{2\alpha_c}{\pi} \right)^{3/4} \exp[ik_{cy}y + ik_{cz}z] \exp[-\alpha|\vec{r} - \vec{r}_j|^2], \quad (5.16)$$

with \vec{r}_j is the center of a modelled harmonic well and a_i, b_i are arbitrary constants in i^{th} region. The WKB approximation is readily applied to the tunnel electrons in the Schottky barrier (i.e. region 2). The wave functions are found to be of the form

$$\psi_2 = a_2 \exp\left[\int_{x_1}^{x_2} \chi_2 dx\right] + b_2 \exp\left[-\int_{x_1}^{x_2} \chi_2 dx\right] \quad (5.17)$$

where $\chi_2(x)$ is magnitude of the complex momentum and x_1, x_2 are the classical turning point. An electron in the metal is represented by a plane wave, which may be written as

$$\psi_3(x) = a_3 \exp[ik_3x] + b_3 \exp[-ik_3x] \quad (5.18)$$

The transmission coefficient T is defined as^[11]

$$T \equiv \left| \frac{J_{trans}}{J_{inc}} \right|$$

where current density is written $J = \frac{\hbar}{2mi} (\psi^* \nabla \psi - \psi \nabla \psi^*)$.

To derive an expression for the transmission coefficient across the barrier, we match these wave functions along with their first derivatives at different boundaries. At the edge of depletion width ($x = x_1$) for $\psi_1(x)$ with $\psi_2(x)$ and at (the contact point) $x = x_2$ for $\psi_2(x)$ with $\psi_3(x)$, we obtain

$$T = \frac{16k_1k_3 \chi_2(x_1) \chi_2(x_2)}{(4\alpha^2(x_1 - x_j)^2 + (k_1^2 + \chi_2^2(x_1))) (k_3^2 + \chi_2^2(x_2))} \exp\left[-\int_{x_1}^{x_2} 2\chi_2(x) dx\right] \quad (5.19)$$

We are concerned with a random system, we must average the result over all random position \vec{r}_j within the volume Ω . If $A(\vec{r}_j)$ is the quantity to be averaged, the average will be

$$\langle A(\vec{r}_j) \rangle = \int \frac{d\vec{r}_j}{\Omega} A(\vec{r}_j) \quad (5.20)$$

The result after averaging eq. (4.19) is

$$\langle T \rangle = T_o(k_1, \chi_2, k_3) \frac{\tan^{-1} \left[\frac{\alpha_c L_x}{\sqrt{2} k_1} \right]}{\alpha_c} \quad (5.21)$$

where

$$T_o(k_1, \chi_2, k_3) = \frac{16k_1 k_3 \chi_2(x_1) \chi_2(x_2)}{L_x \sqrt{2} k_1 (k_1^2 + \chi_2^2(x_1)) (k_3^2 + \chi_2^2(x_2))} \exp \left[- \int_{x_1}^{x_2} 2\chi_2(x) dx \right]$$

When the depletion width (w) can be neglected with respect to the length of specimen in the tunnel direction (L_x). Differentiating the expression for $\langle T \rangle$ leads to

$$\frac{d\langle T \rangle}{d\alpha_c} = \frac{T_o(k_1, \chi_2, k_3)}{\sqrt{2} k_1 L_x \alpha_c \left(1 + \left(\frac{\alpha_c L_x}{\sqrt{2} k_1} \right)^2 \right)} - \frac{T_o(k_1, \chi_2, k_3)}{\alpha_c^2} \tan^{-1} \left(\frac{\alpha_c L_x}{\sqrt{2} k_1} \right) \quad (5.22)$$

Setting eq. (5.22) to be equal to zero, we obtain maximum transmission coefficient when α_c approaches to zero, and is given by

$$T_{\max} = \frac{16k_1k_3 \chi_2(x_1)\chi_2(x_2)}{(k_1^2 + \chi_2^2(x_1))(k_3^2 + \chi_2^2(x_2))} \exp\left[-\int_{x_1}^{x_2} 2\chi_2(x)dx\right] \quad (5.23)$$

This equation is equal to the transmission coefficient of the plane wave incident on to the barrier^[23]. Thus, from eq. (5.21) we obtain

$$\frac{T_{\text{local}}}{T_{\text{delocal}}} = \frac{\sqrt{2}k_c}{L_X \alpha_c} \tan^{-1}\left(\frac{\alpha_c L_X}{\sqrt{2}k_c}\right) \quad (5.24)$$

Here α_c is the energy-dependent Gaussian parameter and k_1 is defined by k_c from as eq. (5.6) (shown in Fig. 5.3). When k_c approaches to zero eq. (5.24) also approaches to zero. In other words, the tunneling transmission coefficient of localized electrons is negligible compared to that of delocalized electrons near the conduction band edge.

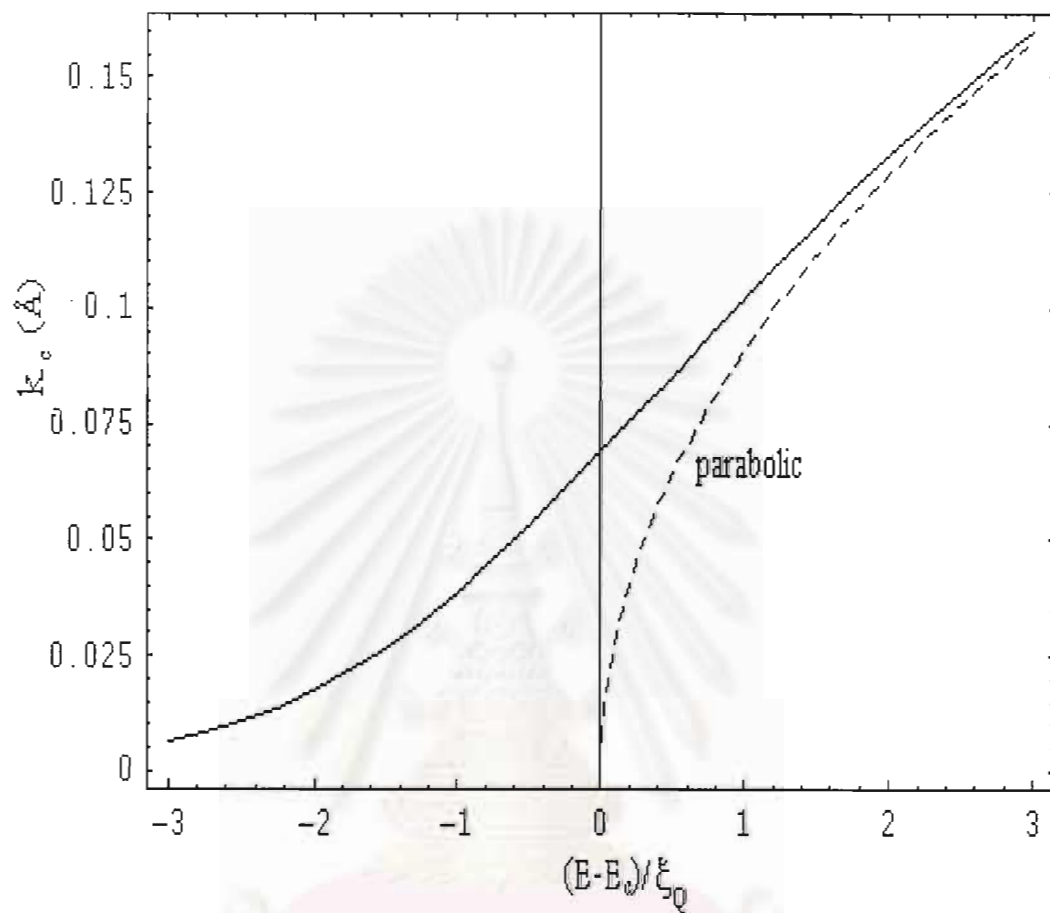


Fig. 5.3 Magnitude of k_c versus arbitrary energies of electrons of n-type GaAs (2×10^{19} donor atoms/cm³) compared to the parabolic relation.

Chapter 6

Summary and Discussion

For a metal contacted with a degenerate semiconductor, especially the semiconductors with small electron effective masses, such as GaAs, the tunneling current will become the dominant transport process, such a mechanism is called “ field emission ”. In more accurately than the depletion approximation, we account for the majority carriers in the charge density and solve Poisson’s equation in case of a degenerate semiconductor. We obtain the electrostatic potential. As a result, based on the field emission, the voltage-current characteristic can be calculated. In this thesis, we are interested in the V-I characteristic at low biases. The influence of the shape of potential barrier on V-I characteristic was considered in Chapter 4. In Chapter 5, we consider the influence of a non-parabolic energy-momentum relationship on the V-I characteristic of a Schottky barrier and compare the localized electron transmission probability with the delocalized electron transmission probability in the last section of Chapter 5.

In chapter 4, we consider a metal contact with a degenerate semiconductor and accounts for the majority carrier in the net charge density. Consequently, the electrostatic potential within the semiconductor is determined by two special cases. Firstly, for lightly degenerate semiconductors, the free carrier density is negligible compared with the donor or acceptor concentration. The electrostatic potential is obtained using the

depletion approximation. Secondly, for highly degenerate semiconductors, we obtained the exponential potential barrier and the temperature as a new parameter of potential barrier.

From eq. (4.5), α increases (i.e., the depletion layer width decreases) as $N_d^{1/6}$ and $T^{-1/2}$. Consequently, the tunneling current will become dominant if the semiconductor is doped heavily or if operated at low temperatures. In other words, the tunneling current dominated at low temperature is obtained by accounting for the majority carrier in the net charge density. In Figs. 4.4, 4.5 and 4.6, show that, the tunneling current density in rectifying increases if the contact barrier decreases, or if the doping concentration and temperature increases, respectively. For highly degenerate semiconductors, the majority carrier cannot be neglected. Thus, the differential contact resistance is smaller than predicted by the depletion approximation (Fig. 4.7) because the exponential barrier approached to the exact barrier.

In chapter 5, the case of n-type GaAs junction, examining of Fig. 5.1 together with the expression for the WKB transmission probability shows that the transmission coefficient of barrier at low biases will be higher, in eq. (5.7), then expected on the basis of the parabolic and Franz's energy-momentum relationship. As a consequence, the current density will increase at low biases (Fig 5.2).

From eq. (5.24), we can show that the tunneling transmission coefficient of the localized electrons is negligible compared to the transmission coefficient of the delocalized electrons near the Fermi level.



สถาบันวิทยบริการ
จุฬาลงกรณ์มหาวิทยาลัย

REFERENCES

- [1] Padovani, F.A. and Stratton, R. "Experimental Energy-Momentum Relationship Determination Using Schottky Barriers," **Phys. Rev. Lett.** 16 (1966): 1202.
- [2] Rhoderik, E.H. and Williams, R.H. **Metal-Semiconductor Contacts**, 2nd ed. Oxford: Clarendon Press, 1988.
- [3] Ferry, D.K. **Semiconductor Physics and Devices**, Oxford: Clarendon Press, 1984.
- [4] Wang, S. **Solid-State Electronic**, 2nd ed. Singapore: John Wiley & Sons, 1977.
- [5] Sritrakool, W., Glyde, H.R., and Sa-yakanit, V. "Absorption near Band Edges in Heavily Doped GaAs," **Phys. Rev. B.**32 (1985): 1090.
- [6] Lundqvist, S., Ranfagni, A., Sa-yakanit, V., and Schulman, L.S. **Path Summation: Achievements and Goals**, Singapore: World Scientific Publishing Co., Pte. Ltd, 1988.
- [7] Kane, E.O. "Thomas-Fermi to Impure Semiconductor Band Structure," **Phys. Rev. B.**131 (1963): 79.
- [8] Sa-yaknit, V. and Glyde, H.R. "Impurity-Band Density of States in Heavily Doped Semiconductors," **Phys. Rev. B.**22 (1980): 6222.

- [9] Sa-yakanit, V., Sritrakool, W., and Glyde H.R. "Imparity-Band Density of States in Heavily doped semiconductors: Numerical results," **Phys. Rev B** 25 (1982): 2776.
- [10] Sze, S.M. **Physics of Semiconductor Devices**, 2nd ed. New Delhi: Wiley Eastern Limited, 1981.
- [11] Liboff, R.L. **Introductory Quantum Mechanics**, 2nd ed. New York : Addisson-Wesley Publishing Company, 1993.
- [12] Merzbacher, E. **Quantum Mechanics**, 3rd ed. New York: John Wiley & Sons, Inc, 1998.
- [13] Shur, M. **Physics of Semiconductor Devices**, New Jersey: Prentice-Hall, Inc. 1990.
- [14] Burstein, E. and Lundqvist, S. **Tunneling Phenomena in Solids**, New York: Plenum Press, 1969:105.
- [15] Padovani, F.A. and Stratton, R. "Field and Thermionic-Field Emission in Schottky Barriers," **Solid-State Electronics** 9 (1996): 695
- [16] Conley, J.W. and Mahan, G.D. "Tunneling Spectroscopy in GaAs" **Phys Rev.** 161 (1967): 681.
- [17] Willardson, R.K. and Baer, A.C. **Semiconductors and Semimetals**, vol.7 New York: Academic Press, 1971.
- [18] Kane, E.O. "Band Structure of Indium Antimonide," **J. Phys. Chem. Solids.** 1 (1957): 249.

- [19] Chang, C.Y. , Fang, Y.K., and Sze, S.M. “Specific Contact Resistance of Metal – Semiconductor Barriers,” **Solid-State Electronics** 14 (1971): 541.
- [20] Seiwatz, R. and Green, M. “Space Charge Calculations for Semiconductors,” **J. Appl. Phys.** 29 (1958): 1034.
- [21] Lou, Y.S. and Wu, C.Y. “The Effects of Impurity Band on the Electrical Characteristic of Metal-Semiconductor Ohmic Contacts” **Solid-State Electronics** 38 (1995): 163.
- [22] Gradshteyn, I.S. and Ryzhik, I.M. **Table of Integrals Series and Products**, 4th ed. New York: Academic Press, 1965.
- [23] Roy, D.K. **Quantum Mechanical Tunneling and Its Applications**, Singapore: World Scientific, 1986.
- [24] Chakraborty, P.K., and Biswas, J. C. “Conduction-Band tailing in Parabolic Band Semiconductors,” **J. Appl. Phys.** 82 (1997): 3328.

CURRICULUM VITAE

Mr. Prathan Srivilai was born on July 27, 1974 in Roi-et. He received his B.Sc. degree in Applied Physics (Solid State Electronics) from King Mongkut 's Institute of Technology Ladkrabang in 1995. During his study for a Master degree he received a grant from the National Science and Technology Development Agency (NSTDA).



สถาบันวิทยบริการ
จุฬาลงกรณ์มหาวิทยาลัย